

COST-AWARE STOPPING FOR BAYESIAN OPTIMIZATION

Qian Xie*

Cornell University

QX66@CORNELL.EDU

Linda Cai*

University of California, Berkeley

TCAI@BERKELEY.EDU

Alexander Terenin

Cornell University

AVT28@CORNELL.EDU

Peter I. Frazier

Cornell University

PF98@CORNELL.EDU

Ziv Scully

Cornell University

ZIVSCULLY@CORNELL.EDU

ABSTRACT

In automated machine learning, scientific discovery, and other applications of Bayesian optimization, deciding when to stop evaluating expensive black-box functions is an important practical consideration. While several adaptive stopping rules have been proposed, in the cost-aware setting they lack guarantees ensuring they stop before incurring excessive function evaluation costs. We propose a *cost-aware stopping rule* for Bayesian optimization that adapts to varying evaluation costs and is free of heuristic tuning. Our rule is grounded in a theoretical connection to state-of-the-art cost-aware acquisition functions, namely the Pandora’s Box Gittins Index (PBGI) and log expected improvement per cost. We prove a theoretical guarantee bounding the expected cumulative evaluation cost incurred by our stopping rule when paired with these two acquisition functions. In experiments on synthetic and empirical tasks, including hyperparameter optimization and neural architecture size search, we show that combining our stopping rule with the PBGI acquisition function usually matches or outperforms other acquisition-function–stopping-rule pairs in terms of *cost-adjusted simple regret*, a metric capturing trade-offs between solution quality and cumulative evaluation cost.

1 INTRODUCTION

Bayesian optimization is a framework designed to efficiently find approximate solutions to optimization problems involving expensive-to-evaluate black-box functions, where derivatives are unavailable. Such problems arise in applications like hyperparameter tuning (Snoek et al., 2012), robot control optimization (Martinez-Cantin, 2017), and material design (Zhang et al., 2020). It works by iteratively, (a) forming a probabilistic model of the black-box objective function based on data collected thus far, then (b) optimizing an acquisition function, which balances exploration-exploitation tradeoffs, to carefully choose a new point at which to observe the unknown function in the next iteration.

In this work, we consider the *cost-aware* setting, where one must pay a cost to collect each data point, and study *adaptive stopping rules* that choose when to stop the optimization process. After stopping at some terminal time, we measure performance in terms of simple regret, which is the difference in value between the best solution found so far and the global optimum. Collecting a data point can reduce simple regret, but incurs cost in order to do so.

As an example, consider using a cloud computing environment to tune the hyperparameters of a classifier in order to optimize a performance metric on a given test set. Training and evaluating test error takes some number of CPU or GPU hours, that may depend on the hyperparameters used. These come with a financial cost, billed by the cloud computing provider, which define our cost function. The objective value is the business value of deploying the trained model under the given hyperparameters—a given function of the model’s accuracy. From this perspective, simple regret can be understood as the opportunity cost for deploying a suboptimal model instead of the optimal one. Motivated by the need to balance cost-performance tradeoff in examples such as above, we aim

*Equal contribution. Correspondence to: Qian Xie <QX66@CORNELL.EDU>.

to design stopping rules that optimizes *expected cost-adjusted simple regret*, defined as the sum of simple regret and the cumulative cost of data collection.

Several stopping rules have been proposed for Bayesian optimization. Simple heuristics—such as fixing a maximum number of iterations or stopping when the best value remains unchanged for a certain number of iterations—are widely used in practice, but can either stop too early or lead to unnecessary evaluations. Other approaches include acquisition-function-based rules that stop when, for instance, the probability of improvement, expected improvement, or knowledge gradient drop below a preset threshold (Lorenz et al., 2015; Nguyen et al., 2017; Frazier & Powell, 2008); and regret-bound-based rules, which use theoretical performance guarantees to decide termination (Makarova et al., 2022; Ishibashi et al., 2023; Wilson, 2024). Most of these target the classical setting which does not explicitly incorporate function evaluation costs.

In this work, we study how to design cost-aware stopping rules, motivated by two primary factors. First, state-of-the-art cost-aware acquisition functions such as the Pandora’s Box Gittins Index (PBGI) (Xie et al., 2024) and log expected improvement per cost (LogEIPC) (Ament et al., 2023) have not yet been studied in the adaptive stopping setting. This is important because—as our experiments in Section 4 will show—for best performance, one should pair different acquisition functions with different stopping rules. Second, while certain stopping rules, such as UCB–LCB (Makarova et al., 2022), are guaranteed to achieve a low simple regret, they are not necessarily guaranteed to do so with low evaluation costs. This is important because—as our experiments will show—UCB–LCB will often incur high evaluation costs, resulting in a high cost-adjusted simple regret.

Our main methodological contribution is a stopping rule that is provably Bayesian-optimal in the independent evaluation case. This stopping rule is constructed based on ideas from Pandora’s Box theory, which forms the theoretical foundation for the recently-proposed PBGI acquisition function. It also aligns closely with an existing stopping rule previously proposed for expected improvement in the classical non-cost-aware setting: when paired with LogEIPC, our proposal extends this stopping rule to the cost-aware setting, thereby establishing a unified approach for cost-aware Bayesian optimization under both kinds of acquisition functions. Our specific contributions are as follows:

1. *A Novel Cost-Aware Stopping Criterion.* We propose an adaptive stopping rule derived naturally from Pandora’s box theory, establishing a unified and principled framework applicable to cost-aware Bayesian optimization.
2. *Theoretical Guarantees.* We prove in Theorem 2 that our stopping rule, when paired with the PBGI or LogEIPC acquisition functions, satisfies a theoretical upper bound on the expected cost-adjusted simple regret, which constitutes the first theoretical guarantee of this type for any adaptive stopping rule for Bayesian optimization.
3. *Empirical Validation.* Our experiments show that combining the PBGI acquisition function with our proposed stopping rule usually matches or outperforms other combinations of acquisition functions and stopping rules.

2 BAYESIAN OPTIMIZATION AND ADAPTIVE STOPPING

In black-box optimization, the goal is to find an approximate optimum of an unknown objective function $f : X \rightarrow \mathbb{R}$ using a limited number of function evaluations at points $x_1, \dots, x_T \in X$ where X is the search space and T is a given search budget, potentially chosen adaptively. The convention measures performance in terms of *expected simple regret* (Garnett, 2023, Sec. 10.1), given by

$$\mathcal{R} = \mathbb{E} \left[\min_{1 \leq t \leq T} f(x_t) - \inf_{x \in X} f(x) \right] \quad (1)$$

where the expectation is taken over all sources of randomness, including the sequence of points x_1, \dots, x_T selected by the algorithm. Bayesian optimization approaches this problem by building a probabilistic model of f —typically a Gaussian process Rasmussen & Williams (2006), conditioned on the observed data points $(x_t, y_t)_{t=1}^T$, where $y_t = f(x_t)$. An acquisition function $\alpha_t : X \rightarrow \mathbb{R}$ then guides the selection of new samples by carefully balancing the exploration-exploitation tradeoff arising from uncertainty about f .

2.1 COST-AWARE BAYESIAN OPTIMIZATION

Cost-aware Bayesian optimization (Lee et al., 2020; Astudillo et al., 2021) extends the above setup to account for the fact that evaluation costs can vary across the search space. For instance, in the hyperparameter tuning example of Section 1, costs can vary according to the time needed to train a machine learning model under a given set of hyperparameters x . Cost-aware Bayesian optimization handles this by introducing a cost function $c : X \rightarrow \mathbb{R}^+$, which may be known or unknown ahead. The cost function, or observed costs, are then used to construct the acquisition function α_t .

In this work, we focus primarily on the *cost-per-sample* formulation (Chick & Frazier, 2012; Cashore et al., 2016; Xie et al., 2024) of cost-aware Bayesian optimization, which seeks methods with stopping time τ , not necessarily fixed, that achieve a low *expected cost-adjusted simple regret*

$$\mathcal{R}_c = \mathbb{E} \left[\underbrace{\min_{1 \leq t \leq \tau} f(x_t) - \inf_{x \in X} f(x)}_{\text{simple regret}} + \underbrace{\sum_{t=1}^{\tau} c(x_t)}_{\text{cumulative cost}} \right]. \quad (2)$$

One can also work with the *expected budget-constrained* formulation (Xie et al., 2024), which incorporates budget constraints explicitly, and seeks algorithms which achieve a low simple regret under an expected evaluation budget. Here, performance is evaluated in terms of

$$\mathcal{R} = \mathbb{E} \left[\min_{1 \leq t \leq \tau} f(x_t) - \inf_{x \in X} f(x) \right] \quad \text{where } x_1, \dots, x_\tau \text{ satisfy } \mathbb{E} \sum_{t=1}^{\tau} c(x_t) \leq B. \quad (3)$$

The stopping rules we study can be applied in this setting as well: we discuss this in Section 3.1.

For both settings, we work with a few acquisition functions—chiefly, *log expected improvement per cost (LogEIPC)* (Ament et al., 2023) and the *Pandora’s Box Gittins Index (PBGI)* (Xie et al., 2024):

$$\alpha_t^{\text{LogEIPC}}(x) = \log \frac{\text{EI}_{f|x_{1:t}, y_{1:t}}(x; y_{1:t}^*)}{c(x)} \quad (4)$$

and

$$\alpha_t^{\text{PBGI}}(x) = \begin{cases} g & \text{where } g \text{ solves } \text{EI}_{f|x_{1:t}, y_{1:t}}(x; g) = c(x), \quad x \notin \{x_1, \dots, x_t\} \\ f(x), & x \in \{x_1, \dots, x_t\} \end{cases} \quad (5)$$

where $y_{1:t}^* = \min_{1 \leq s \leq t} y_s$ is the best value observed in the first t steps, and $\text{EI}_\psi(x; y) = \mathbb{E}[\max(y - \psi(x), 0)]$ is the expected improvement at point x with respect to some random function $\psi : X \rightarrow \mathbb{R}$ and a baseline value y . In the uniform-cost setting, we also consider the classical *lower confidence bound* and *Thompson sampling* acquisition functions; see Garnett (2023) for details.

2.2 ADAPTIVE STOPPING RULES

To the best of our knowledge, stopping rules for Bayesian optimization typically do not incorporate cost explicitly into the stopping criterion. We broadly categorize existing methods as follows:

1. *Criteria based on convergence or significance of improvement.* This includes empirical convergence, namely stopping when the best value remains unchanged for a fixed number of iterations, or the *global stopping strategy (GSS)* (Bakshy et al., 2018), which stops when the improvement is no longer statistically significant relative to the inter-quartile range (i.e., the range between the 25th percentile and the 75th percentile) of prior observations. In the multi-fidelity setting, Foumani & Bostanabad (2025) proposed stopping when the high-fidelity surrogate’s estimated optimum has stabilized over a window of iterations, which is related to cost-awareness but differs from our setting with explicitly varying evaluation costs.
2. *Acquisition-based criteria.* This includes stopping rules built from acquisition functions such as the *probability of improvement (PI)* (Lorenz et al., 2015), *expected improvement (EI)* (Locatelli, 1997; Nguyen et al., 2017; Ishibashi et al., 2023), and *knowledge gradient (KG)* (Frazier & Powell, 2008). These approaches typically stop when the acquisition value falls below a fixed threshold—a predetermined constant, median of the initial acquisition values, or the cost of sampling—but typically assume uniform costs and do not adapt to evaluation costs which can vary across the search space.

3. *Regret-based criteria.* This includes stopping rules based on confidence bounds such as UCB-LCB (Makarova et al., 2022) and the *gap of expected minimum simple regrets* (Ishibashi et al., 2023). These stop when certain estimated regret bounds fall below a preset or data-driven threshold. The related *probabilistic regret bound (PRB)* stopping rule (Wilson, 2024) stops when estimated simple regret is below a small threshold ϵ with confidence $1 - \delta$.

In settings beyond Bayesian optimization, Chick & Frazier (2012) have proposed a cost-aware stopping rules for finite-domain sequential sampling problems with independent values. Although this formulation allows for varying costs, it does not extend to general Bayesian optimization settings which use correlated Gaussian process models.

3 A STOPPING RULE BASED ON THE PANDORA’S BOX GITTINS INDEX

In this work, we propose a new stopping rule tailored for two state-of-the-art acquisition functions used in cost-aware Bayesian optimization: LogEIPC and PBGI, introduced in Section 2. As discussed by Xie et al. (2024), these acquisition functions are closely connected, arising from two different approximations of the intractable dynamic program which defines the Bayesian-optimal policy for cost-aware Bayesian optimization. We now show that this connection can be used to obtain a principled stopping criterion to be paired with both acquisition functions.

A stopping rule for PBGI. To derive a stopping rule for PBGI, consider first the Pandora’s Box problem, from which it is derived. Pandora’s Box can be seen as a special case of cost-per-sample Bayesian optimization, as introduced in Section 2, where $X = \{1, \dots, N\}$ is a discrete space and f is assumed uncorrelated. In this setting, the observed values do not affect the posterior distribution—meaning, we have $f(x') \mid x_{1:t}, y_{1:t} = f(x')$ at all unobserved points x' —and thus the acquisition function value at point x is time-invariant and can be written simply as $\alpha^{\text{PBGI}}(x)$, where $\text{EI}_f(x; \alpha^{\text{PBGI}}(x)) = c(x)$. Following Weitzman (1979), one can show using a Gittins index argument that selecting x_t to minimize α^{PBGI} is Bayesian-optimal under minimization—the algorithm which does so achieves the smallest expected cost-adjusted simple regret, among all adaptive algorithms.

One critical detail applied in the optimality argument of Weitzman (1979) is that the policy defined by α^{PBGI} is *not* Bayesian-optimal for any fixed deterministic T . Instead, it is optimal only when the stopping time T is chosen according to the condition

$$\min_{x \in X \setminus \{x_1, \dots, x_t\}} \alpha^{\text{PBGI}}(x) \geq y_{1:t}^*, \quad (6)$$

where \geq can be replaced by $>$ ¹, and as before, $y_{1:t}^*$ is the best value observed so far.

In the correlated setting we study, Xie et al. (2024) extend α^{PBGI} to define an acquisition function by recomputing it at each time step t based on the posterior mean and variance, which defines α_t^{PBGI} as in (5). In order to also extend the associated stopping rule, a subtle design choice arises: should we use $\alpha_{t-1}^{\text{PBGI}}$ (before update) or α_t^{PBGI} (after update) in (6)? While prior theoretical work (Gergatsouli & Tzamos, 2023) adopts the former choice, we instead propose the latter, for two main reasons.

First, we argue it more faithfully reflects the intuition behind Weitzman’s original stopping rule. In the independent setting, $\alpha^{\text{PBGI}}(x)$ represents a kind of *fair value* for point x (Kleinberg et al., 2016). For evaluated points $x \in \{x_1, \dots, x_t\}$, this is simply the observed function value. For unevaluated points $x \notin \{x_1, \dots, x_t\}$, the fair value reflects uncertainty in $f(x)$ and the cost $c(x)$. The stopping rule (6) then says to *stop when the best fair value is among the already-evaluated points*—namely, when no point provides positive expected gain relative to its cost if evaluated in the next round, conditioned on current observations. In the correlated setting, the fair value naturally extends to α_t^{PBGI} , because this incorporates all known information at a given time. Second, we show in Appendix D.2 that using α_t^{PBGI} yields tangible empirical gains in cost-adjusted regret.

Connection with LogEIPC. The above reasoning may at first seem to be fundamentally tied to the Pandora’s Box problem and its Gittins-index-theoretic properties. We now show that it admits a

¹Following Xie et al. (2024, Appendix B), optimality holds under any tie-breaking rule in the cost-per-sample setting, but only under a carefully-chosen stochastic tie-breaking rule in the expected budget-constrained setting. For simplicity, we use the stopping-as-early-as-possible tie-breaking rule throughout this paper.

second interpretation in terms of log expected improvement per cost, which arises from a completely different one-time-step approximation to the Bayesian-optimal dynamic program for cost-aware Bayesian optimization in the general correlated setting.

To show this, we start with definitions above, and apply a sequence of transformations. For any unevaluated point $x \in X \setminus \{x_1, \dots, x_t\}$, recall that $\alpha_t^{\text{PBGI}}(x)$ is defined in (5) to be the solution to

$$\text{EI}_{f|x_{1:t}, y_{1:t}}(x; \alpha_t^{\text{PBGI}}(x)) = c(x) \quad (7)$$

and since $\text{EI}_\psi(x; y)$ is strictly increasing in y , any inequality involving $\alpha_t^{\text{PBGI}}(x; c)$ can be lifted through the EI function without changing its direction, which means

$$\alpha_t^{\text{PBGI}}(x) \geq y_{1:t}^* \quad \text{holds if and only if} \quad \text{EI}_{f|x_{1:t}, y_{1:t}}(x; y_{1:t}^*) \leq c(x). \quad (8)$$

This implies that the PBGI stopping rule from (6) is equivalent to stopping when

$$\text{EI}_{f|x_{1:t}, y_{1:t}}(x; y_{1:t}^*) \leq c(x) \quad \text{for all } x \in X \setminus \{x_1, \dots, x_t\}. \quad (9)$$

meaning *stop when no point's expected improvement is worth its evaluation cost*. Rearranging the inequality and taking logs, we can rewrite this condition using the LogEIPC acquisition function²:

$$\max_{x \in X \setminus \{x_1, \dots, x_t\}} \alpha_t^{\text{LogEIPC}}(x; y_{1:t}^*) \leq 0. \quad (10)$$

We call the stopping rule given by the equivalent conditions (6), (9), and (10) the *PBGI/LogEIPC stopping rule*. Figure 1 gives an illustration of how the rule behaves in a simple setting, demonstrating that it is more conservative—preferring to stop earlier—when the cost is high.

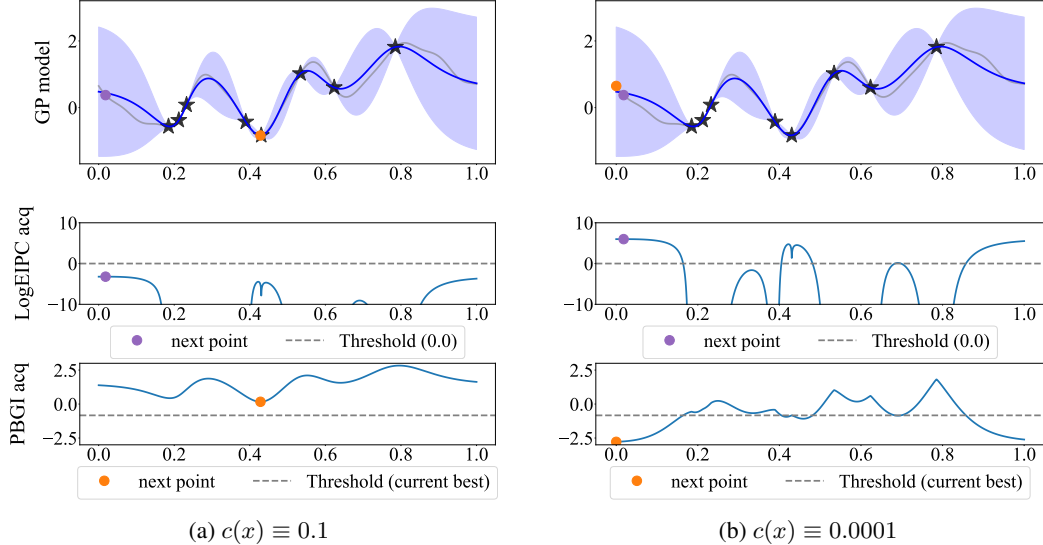


Figure 1: Illustration of the PBGI/LogEIPC stopping rule under a uniform-cost setting. When the cost-per-sample is large ($c(x) \equiv 0.1$), the maximum LogEIPC acquisition value falls below the threshold 0.0 and the minimum PBGI acquisition value exceeds the current best observed value, indicating stopping; when the cost-per-sample is small ($c(x) \equiv 0.0001$), the maximum LogEIPC acquisition value remains above the threshold 0.0 and the minimum PBGI acquisition value is smaller than the current best observed value, indicating no stopping.

3.1 THEORETICAL GUARANTEES ON COST-ADJUSTED SIMPLE REGRET

The connection between PBGI and LogEIPC in fact goes beyond a shared stopping rule. In Lemma 1, we prove that when paired with this stopping rule, both acquisition functions guarantee that at each iteration before stopping, the expected improvement at the selected point is at least its evaluation cost.

²Excluding evaluated points is not theoretically required but often beneficial in practice, as numerical stability adjustments can cause their expected improvement to remain positive.

Lemma 1. Let X be compact, and let $f : X \rightarrow \mathbb{R}$ be a random function with constant mean μ . Consider a Bayesian optimization algorithm that begins at some initial point $x_1 \in X$ with cost $C = c(x_1)$, acquires additional points using either the PBGI or LogEIPC acquisition function, and uses the PBGI/LogEIPC stopping rule. Let $\tau = \min_{t \geq 1} \{\sup_{x \in X} \alpha_t^{\text{LogEIPC}}(x) < 0\}$ be the algorithm's stopping time, and denote the posterior expected improvement function by $\alpha_t^{\text{EI}}(x) = \text{EI}_{f|x_{1:t}, y_{1:t}}(x; y_{1:t}^*)$. Then, $\alpha_t^{\text{EI}}(x_{t+1}) \geq c(x_{t+1})$ for all $t < \tau$.

Proofs are in Appendix B. As a consequence of this claim, we show in Theorem 2 that the PBGI/LogEIPC stopping rule, when paired with PBGI or LogEIPC, achieve strictly better cost-adjusted simple regret than the naive strategy of stopping immediately after the initial evaluation. While this may sound obvious, many acquisition function–stopping rule pairs fail to satisfy this *no-worse-than-immediate* property in practice (see Figures 2 to 4), largely because most stopping rules are designed with simple regret alone in mind and do not explicitly account for evaluation costs. To our knowledge, this is the first result establishing a formal guarantee on cost-adjusted simple regret for Bayesian optimization, generalizing beyond simpler settings such as Pandora’s Box, which assumes independent and discrete evaluations.

Theorem 2. Consider the setting, acquisition function, and stopping rule specified in Lemma 1. Let $U = \mu - \mathbb{E}[\min_{x \in X} f(x)] < \infty$, then the algorithm’s expected cost-adjusted simple regret is bounded by

$$\mathbb{E} \left[y_{1:\tau}^* - \min_{x \in X} f(x) + \sum_{t=1}^{\tau} c(x_t) \right] \leq \mathbb{E} \left[\underbrace{y_1 - \min_{x \in X} f(x) + c(x_1)}_{\text{cost-adjusted regret of immediate stopping}} \right] = U + C. \quad (11)$$

3.1.1 IMPLICATION IN THE BUDGET-CONSTRAINED SETTING

We first note that in the discrete Pandora’s Box setting, under an expected budget constraint B , minimizing $\alpha_t^{\text{PBGI}}(x)$ is Bayesian-optimal: it achieves the lowest *expected simple regret, among all algorithms* satisfying $\mathbb{E}[\sum_{t=1}^{\tau} c(x_t)] \leq B$, and the cost function used in defining $\alpha_t^{\text{PBGI}}(x)$ is $\lambda c(x)$ for some cost-scaling factor λ which depends on B (Xie et al., 2024, Theorem 2).

This result, at first, appear to be completely Pandora’s-Box-theoretic: it requires X to be discrete and f to be independent. In the more general correlated setting of cost-aware Bayesian optimization, however, Bayesian optimality of PBGI may no longer hold, and the relationship between B and the choice of λ is not immediately clear. Theorem 2 helps bridge this gap: it provides an upper bound on the expected cumulative cost up to the stopping time, which in turn yields the following principled choice of λ that ensures compliance with the budget constraint.

Corollary 3. Consider the setting, acquisition function, stopping rule, and notation specified in Lemma 1 and Theorem 2, but with costs rescaled by a factor $\lambda > 0$: both acquisition values and stopping conditions are computed using $\lambda c(\cdot)$. If the cost-scaling factor is set to $\lambda = \frac{U}{B-C}$, then the algorithm’s expected cumulative unscaled cost satisfies $\mathbb{E}[\sum_{t=1}^{\tau} c(x_t)] \leq B$.

If this choice of λ proves overly conservative—leading to underspending within the budget—it can be paired with the PBGI-D variant of Xie et al. (2024), which starts with $\lambda = \lambda_0$ and halves it each time stopping is triggered. Choosing $\lambda_0 = U/(B - C)$ aligns the initial fixed- λ phase with the budget in expectation, while ensuring that the adaptive decay is activated as designed. In Figure 11 in Appendix D, we show PBGI-D with this choice of λ_0 is competitive.

3.2 PRACTICAL IMPLEMENTATION CONSIDERATIONS FOR PBGI/LOGEIPC STOPPING RULE

Expressing objective and cost in common units. Evaluation costs are often measured in different units than the objective, such as time versus accuracy. To compare them directly, we rescale costs by a constant $\lambda > 0$, the conversion rate between cost and objective improvement. For instance, if one is willing to spend 1000 seconds to reduce test error by 0.01, then $\lambda = 10^{-5}$. Importantly, in the cost-per-sample setting we mainly study, λ is set by the problem provider rather than tuned by the user, whereas the budgeted setting without a natural unit conversion is discussed in Section 3.1.1.

Unknown costs. In practice, evaluation costs are often not known in advance. They can be modeled either (i) deterministically, using domain knowledge (e.g., proportional to model size in

hyperparameter tuning), or (ii) stochastically, via a Gaussian process over log costs. In Section 4, we present empirical benchmark results under both modeling approaches. For the stochastic approach, we follow Astudillo et al. (2021, Proposition 2) to model $\ln c(x)$ as a Gaussian process with posterior mean $\mu_{\ln c}$ and variance $\sigma_{\ln c}^2$. To compute LogEIPC or PBGI, as well as their related stopping rules (including prior acquisition-based ones and ours), we replace $c(x)$ in Equations (4), (5) and (9) with $\mathbb{E}[c(x)] = \exp(\mu_{\ln c}(x) + (\sigma_{\ln c}(x))^2/2)$. See Appendix D.3 for further discussion.

Preventing spurious stops. Although our stopping rule has theoretical guarantees, in practice, it—like other adaptive stopping rules—can still suffer from spurious stops caused by two main sources which we now discuss. First, early in the optimization process, the Gaussian process model parameters often fluctuate significantly as new data points are collected, causing unstable stopping signals. To mitigate this, we enforce a stabilization period consisting of the first several evaluations, during which we do not allow any stopping rule to trigger. Second, imperfect optimization of the acquisition function—which is especially common in higher-dimensional search spaces—can lead to misleading stopping signals. To handle this, we use a *debounce* strategy, requiring the stopping rule to consistently indicate stopping over several consecutive iterations before stopping optimization.

4 EXPERIMENTS

To evaluate our proposed PBGI/LogEIPC stopping rule, we design three complementary sets of experiments that progressively test its performance. First, we consider an idealized, low-dimensional Bayesian regret setting in which the Gaussian process model exactly matches the true objective. This controlled environment allows us to isolate the effect of different stopping rules without interference from modeling or optimization errors. Then, we move to a higher-dimensional Bayesian regret setting where each acquisition-function minimization must be approximated via a numerical optimizer. Finally, we test in practical scenarios with potential objective model mismatch, using the LCBench hyperparameter tuning benchmark and the NATS neural architecture size search benchmark. In each case, we compare pairs of acquisition functions and stopping rules, which we describe next.

Acquisition functions. We consider four common acquisition functions that were discussed in Section 2: *log expected improvement per cost (LogEIPC)*, *Pandora’s Box Gittins Index (PBGI)*, *lower confidence bound (LCB)*, and *Thompson sampling (TS)*—chosen for their competitive performance, computational efficiency, and close connections to existing stopping rules.

Baselines. We compare the proposed PBGI/LogEIPC stopping rule against several stopping rules from prior work: *UCB–LCB* Makarova et al. (2022), *LogEIPC-med* Ishibashi et al. (2023), *SRGap-med* Ishibashi et al. (2023), and *PRB* Wilson (2024). We also include two simple heuristics used in practice: *Convergence* and *GSS*. *UCB–LCB* stops once the gap between upper and lower confidence bounds falls below a configurable threshold θ . *LogEIPC-med* stops when the log expected improvement per cost drops beneath $\log(\eta)$ plus the median of its initial I values. *SRGap-med* stops when the gap of the expected minimum simple regret falls below χ times the median of its initial I values. *PRB* triggers once a probabilistic regret bound satisfies the regret tolerance ϵ and confidence δ parameters. *Convergence* stops as soon as the best observed value remains unchanged for w iterations. *GSS* stops if the recent improvement is less than $\phi \times \text{IQR}$ over the past w trials where IQR denotes the inter-quartile range of current observations. Finally, we include two reference baselines: *Immediate*, which stops right after the initial evaluation (see Section 3.1), and *Hindsight*, which, for each trial, selects the stopping time that yields the lowest cost-adjusted simple regret in hindsight, thus providing a lower bound on achievable performance.

In our experiments, unless specified otherwise, we follow parameter values recommended in the literature, and set $\theta = 0.01$, $\eta = 0.01$, $\chi = 0.01$, $I = 20$, $\epsilon = 0.1$ for Bayesian regret experiments, $\epsilon = 0.5\%$ of the best test error for empirical experiments, $\delta = 0.05$, $w = 5$, and $\phi = 0.01$. Each experiment is repeated with 50 random seeds to assess variability, and we report the mean with error bars (2 times the standard error) for each stopping rule. Each trial, in the sense of a run with a distinct random seed, is capped at a fixed number of iterations; if a stopping rule is not triggered within this limit, the stopping time is set to the cap. Details are provided in Appendix C.

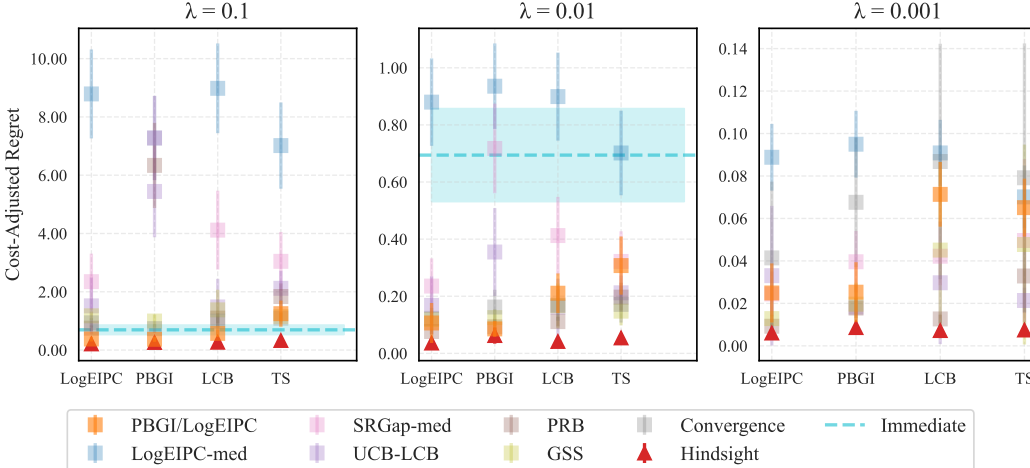


Figure 2: Cost-adjusted simple regret across acquisition-stopping rule pairs in 1D Bayesian regret setting. Objectives are sampled from a GP with Matérn-5/2 kernel, with a linear cost function scaled by $\lambda = 0.1, 0.01, 0.001$. Matched PBGI pairs perform the best at $\lambda = 0.1, 0.01$, and remain close to hindsight-optimal at $\lambda = 0.001$, though slightly outperformed by PRB and GSS paired with PBGI. The Immediate baseline is omitted at $\lambda = 0.001$ due to its significantly higher regret (mean: 0.6942, error bar: [0.5314, 0.8570]) compared to other stopping rules.

4.1 BAYESIAN REGRET

We first evaluate our PBGI/LogEIPC stopping rule on random functions sampled from prior. Specifically, objective functions are sampled from Gaussian processes with Matérn 5/2 kernels with length scale 0.1, defined over spaces of dimension $d = 1$ and $d = 8$. We consider a variety of evaluation cost function types, including uniform costs, linearly increasing costs in terms of parameter magnitude, and periodic costs that vary non-monotonically over the domain.

In the 1-dimensional experiments, we perform an exhaustive grid search over $[0, 1]$ to isolate the effect of stopping behavior from numerical optimization. In the 8-dimensional setting, due to instability from higher dimensionality, we apply moving average with a window size of 20 when computing the PBGI/LogEIPC stopping condition. See Figure 5 in Appendix C for an illustration. More details on our experiment setup, and computational considerations are provided in Appendices C and D.

Figure 2 shows a comparison of cost-adjusted regret for acquisition function and stopping rule pairings under different cost-scaling factors λ in the 1-dimensional setting. From the plot, our PBGI/LogEIPC stopping rule pairing with LogEIPC or PBGI acquisition function delivers competitive performance for each λ , and is particularly strong in handling high-cost scenarios—those with large λ .

In the 1-dimensional setting, the Bayesian optimization problem is relatively straightforward and all acquisition functions attain nearly identical hindsight optima, independent of cost scale or cost type. In the 8-dimensional experiments, however, clear gaps emerge: Figure 3 compares cost-adjusted regret under uniform, linear, and periodic cost regimes. Under uniform and linear costs, LogEIPC, PBGI, and LCB perform similarly and substantially outperform TS, while in the periodic case, LogEIPC and PBGI outperform LCB and TS. In every case, combining our stopping rule with the LogEIPC, PBGI, or LCB acquisition function yields cost-adjusted regret nearly matching the hindsight optimal. This shows our PBGI/LogEIPC stopping rule to be relatively robust against challenges in acquisition function optimization. Further discussions of our experiments across all cost types and cost-scaling factors can be found in Appendix D.

4.2 EMPIRICAL AUTOMATED MACHINE LEARNING BENCHMARKS

We then evaluate on two empirical benchmarks based on use cases from hyperparameter optimization and neural architecture search: LCbench (Zimmer et al., 2021) and NATS-Bench (Dong et al., 2021).

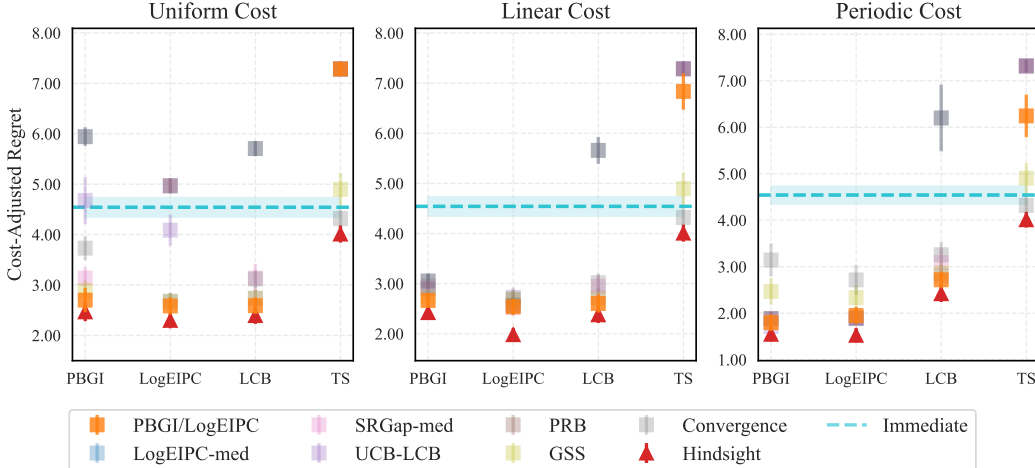


Figure 3: Cost-adjusted simple regret across acquisition–stopping rule pairs in 8D Bayesian regret experiments. Objectives are sampled from a GP with a Matérn-5/2 kernel, using three different cost functions scaled by $\lambda = 0.01$. Our PBGI/LogEIPC stopping rule consistently yields the lowest cost-adjusted regret that is close to hindsight optimal, when paired with LogEIPC, PBGI, and LCB.

LCBench provides training data of 2,000 hyperparameter configurations evaluated on multiple OpenML datasets. Due to the space constraints, we report results on the first three datasets from the lite version, covering image, mixed-type tabular, and large-scale numerical tabular classification tasks. In the *unknown-cost* experiments, the cost is the full (200-epoch) training time. For the known-cost setting, we observe that training time to scale approximately linearly with the number of model parameters. Based on a linear regression fit (see Appendix C), we adopt $10^{-3} \times p$, where p is the number of model parameters, as a proxy of training time.

NATS-Bench provides a search space of 32,768 neural architectures varying in channel sizes across layers, evaluated on three datasets. As in LCBench, for the known-cost experiments, we approximate the full runtime (training + validation time) at 90 epochs using $\alpha F + \beta$, where F is the number of floating point operations; see Appendix C for details.

We report the mean and error bars (2 times standard error) of the *cost-adjusted simple regret*, where we consider the evaluation costs to be some representative cost-scaling factor λ (see Section 3.2) multiplied with cumulative runtime. Simple regret is computed as the difference between (a) test error of the configuration with best validation error at the stopping time and (b) the best test error over all configurations. We present the results using proxy runtime here, and defer to Appendix D the additional results under (i) the *cost model mismatch* scenario (proxy runtime used during Bayesian optimization but actual runtime used for evaluation), and (ii) the *unknown-cost* scenario (actual runtime used during Bayesian optimization).

Figure 4 presents cost-adjusted regret for pairs of acquisition function and stopping rule on classification tasks from LCBench and NATS-Bench, with representative³ cost-scaling factor $\lambda = 10^{-4}$ and $\lambda = 10^{-5}$ respectively. Additional results under different cost-scaling factors and the unknown-cost setting are provided in Figures 15 to 17 of Appendix D, along with visual comparisons between adaptive and fixed-iteration stopping. Overall, our PBGI/LogEIPC stopping rule consistently performs strongly in terms of cost-adjusted simple regret, particularly when paired with the PBGI acquisition function. We also report, in Table 1 of Appendix D, how often each stopping rule fails to trigger within the 200-iteration cap: baselines such as SRGap-med and UCB–LCB often fail to stop early—particularly on NATS-Bench—whereas our stopping rule reliably stops before the cap.

As we transition from model match to model mismatch, where the true objective function does not align perfectly with the Gaussian process prior, we find that our stopping rule, when paired with the

³These were chosen to avoid degenerate cases—neither so large that the policy stops after only a few evaluations (e.g., $\lambda = 10^{-4}$ on NATS-Bench, Figure 18) nor so small that evaluations are effectively free.

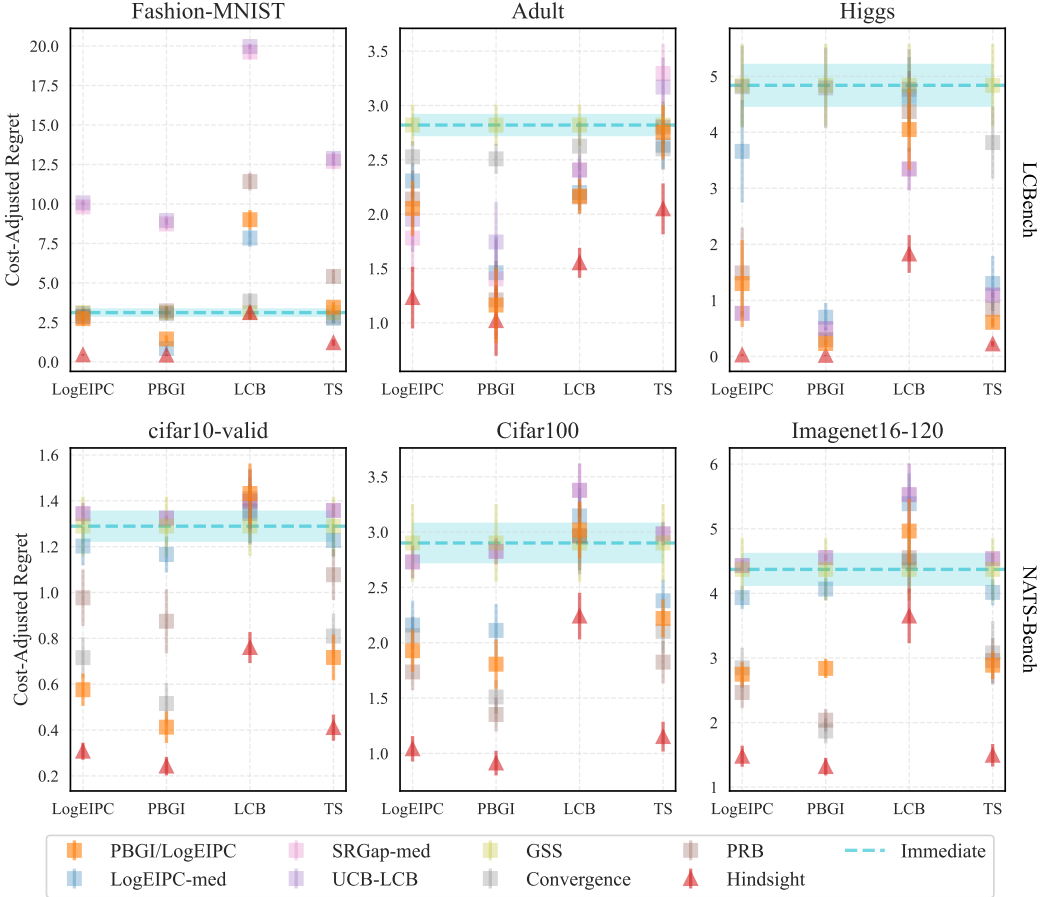


Figure 4: Comparison of cost-adjusted simple regret across acquisition function and stopping rule pairs on LCBench and NATS-Bench. The objective is to minimize validation error on classification tasks, with proxy runtime as evaluation cost, scaled by representative values of λ (10^{-4} for LCBench and 10^{-5} for NATS-Bench); see Figures 12 to 14 for performance under other λ . The matched PBGI combination performs best on *adult*, *higgs*, and *cifar10-valid*, second-best on *Fashion-MNIST*, and third-best on the remaining two, while closely approaching the hindsight optimal across all tasks. Our stopping rule is also competitive when paired with LogEIPC or TS.

PBGI acquisition function, continues to deliver performance close to the hindsight optimal, except on two NATS datasets likely affected by severe mismatch. In contrast, pairing with the LogEIPC acquisition function is less competitive. This degradation appears to stem from the relative advantage of PBGI over LogEIPC in higher dimensions or misspecified settings: as shown in Figure 11 in Appendix D, PBGI maintains stronger performance under misspecification, thus contributing to the improved overall cost-adjusted regret. Thus, while our stopping rule is broadly robust, the choice of acquisition function remains an important consideration when facing objective model mismatch.

5 CONCLUSION

We develop the *PBGI/LogEIPC stopping rule* for Bayesian optimization with varying evaluation costs. Paired with either the PBGI or LogEIPC acquisition function, it (a) satisfies a theoretical guarantee bounding the expected cost-adjusted simple regret (Section 3.1), and (b) shows strong empirical performance in terms of cost-adjusted simple regret (Section 4). We believe our framework can be extended to settings involving noisy, multi-fidelity or batched evaluations, as well as alternative objective formulations—for instance, applying a sigmoid transformation to test error rather than a linear one, to reflect real-world user preferences that shift sharply once error falls below a threshold.

ACKNOWLEDGMENTS

QX thanks Nairen Cao for helpful discussions on hindsight optimal, Theodore Brown for helpful discussions on LCBench runtime proxy, and Raul Astudillo for helpful discussions on unknown cost handling for LogEIPC. AT thanks James T. Wilson for helpful comments on stopping rules for Bayesian optimization. LC is funded by the European Union (ERC-2022-SYG-OCEAN-101071601). Views and opinions expressed are however those of the author(s) only and do not necessarily reflect those of the European Union or the European Research Council Executive Agency. Neither the European Union nor the granting authority can be held responsible for them. AT was supported by Cornell University, jointly via the Center for Data Science for Enterprise and Society, the College of Engineering, and the Ann S. Bowers College of Computing and Information Science. PF was supported by AFOSR FA9550-20-1-0351. ZS was supported by the NSF under grant no. CMMI-2307008.

REFERENCES

- Sebastian Ament, Samuel Daulton, David Eriksson, Maximilian Balandat, and Eytan Bakshy. Unexpected improvements to expected improvement for bayesian optimization. *Advances in Neural Information Processing Systems*, 36:20577–20612, 2023.
- Raul Astudillo, Daniel Jiang, Maximilian Balandat, Eytan Bakshy, and Peter I Frazier. Multi-step budgeted bayesian optimization with unknown evaluation costs. In *Advances in Neural Information Processing Systems*, 2021.
- Eytan Bakshy, Lili Dworkin, Brian Karrer, Konstantin Kashin, Benjamin Letham, Ashwin Murthy, and Shaun Singh. Ae: A domain-agnostic platform for adaptive experimentation. In *Conference on neural information processing systems*, pp. 1–8, 2018.
- Maximilian Balandat, Brian Karrer, Daniel Jiang, Samuel Daulton, Ben Letham, Andrew G Wilson, and Eytan Bakshy. Botorch: A framework for efficient monte-carlo bayesian optimization. *Advances in neural information processing systems*, 33:21524–21538, 2020.
- J Massey Cashore, Lemuel Kumarga, and Peter I Frazier. Multi-step bayesian optimization for one-dimensional feasibility determination. *arXiv preprint arXiv:1607.03195*, 2016.
- Stephen E Chick and Peter Frazier. Sequential sampling with economics of selection procedures. *Management Science*, 58(3):550–569, 2012.
- Xuanyi Dong, Lu Liu, Katarzyna Musial, and Bogdan Gabrys. Nats-bench: Benchmarking nas algorithms for architecture topology and size. *IEEE transactions on pattern analysis and machine intelligence*, 44(7):3634–3646, 2021.
- Zahra Zanjani Foumani and Ramin Bostanabad. Constrained multi-fidelity bayesian optimization with automatic stop condition. *Corr*, abs/2503.01126, 2025. doi: 10.48550/ARXIV.2503.01126. URL [HTTPS://DOI.ORG/10.48550/ARXIV.2503.01126](https://doi.org/10.48550/ARXIV.2503.01126).
- Peter Frazier and Warren B Powell. The knowledge-gradient stopping rule for ranking and selection. In *2008 Winter Simulation Conference*, pp. 305–312. IEEE, 2008.
- Roman Garnett. *Bayesian optimization*. Cambridge University Press, 2023.
- Evangelia Gergatsouli and Christos Tzamos. Weitzman’s rule for pandora’s box with correlations. *Advances in Neural Information Processing Systems*, 36:12644–12664, 2023.
- Shouri Hu, Haowei Wang, Zhongxiang Dai, Bryan Kian Hsiang Low, and Szu Hui Ng. Adjusted expected improvement for cumulative regret minimization in noisy bayesian optimization. *Journal of Machine Learning Research*, 26(46):1–33, 2025.
- Hideaki Ishibashi, Masayuki Karasuyama, Ichiro Takeuchi, and Hideitsu Hino. A stopping criterion for bayesian optimization by the gap of expected minimum simple regrets. In *International Conference on Artificial Intelligence and Statistics*, pp. 6463–6497. PMLR, 2023.

- Robert Kleinberg, Bo Waggoner, and E Glen Weyl. Descending price optimally coordinates search. *arXiv preprint arXiv:1603.07682*, 2016.
- Eric Hans Lee, Valerio Perrone, Cedric Archambeau, and Matthias Seeger. Cost-aware bayesian optimization. In *ICML Workshop on Automated Machine Learning*, 2020.
- Mikhail Lifshits. Lectures on gaussian processes. In *Lectures on Gaussian Processes*, pp. 1–117. Springer, 2012.
- Marco Locatelli. Bayesian algorithms for one-dimensional global optimization. *Journal of Global Optimization*, 10:57–76, 1997.
- Romy Lorenz, Ricardo P Monti, Ines R Violante, Aldo A Faisal, Christoforos Anagnostopoulos, Robert Leech, and Giovanni Montana. Stopping criteria for boosting automatic experimental design using real-time fmri with bayesian optimization. *arXiv preprint arXiv:1511.07827*, 2015.
- Anastasia Makarova, Huibin Shen, Valerio Perrone, Aaron Klein, Jean Baptiste Faddoul, Andreas Krause, Matthias Seeger, and Cedric Archambeau. Automatic termination for hyperparameter optimization. In *International Conference on Automated Machine Learning*, pp. 7–1. PMLR, 2022.
- Ruben Martinez-Cantin. Bayesian optimization with adaptive kernels for robot control. In *International Conference on Robotics and Automation*, 2017.
- Vu Nguyen, Sunil Gupta, Santu Rana, Cheng Li, and Svetha Venkatesh. Regret for expected improvement over the best-observed value and stopping condition. In *Asian conference on machine learning*, pp. 279–294. PMLR, 2017.
- Carl Edward Rasmussen and Christopher KI Williams. *Gaussian Processes for Machine Learning*. Cambridge University Press, 2006.
- Jasper Snoek, Hugo Larochelle, and Ryan P Adams. Practical bayesian optimization of machine learning algorithms. *Advances in Neural Information Processing Systems*, 2012.
- Niranjan Srinivas, Andreas Krause, Sham M Kakade, and Matthias Seeger. Gaussian process optimization in the bandit setting: No regret and experimental design. *arXiv preprint arXiv:0912.3995*, 2009.
- Martin L Weitzman. Optimal search for the best alternative. *Econometrica*, 1979.
- James Wilson. Stopping bayesian optimization with probabilistic regret bounds. *Advances in Neural Information Processing Systems*, 37:98264–98296, 2024.
- Qian Xie, Raul Astudillo, Peter Frazier, Ziv Scully, and Alexander Terenin. Cost-aware bayesian optimization via the pandora’s box gittins index. *Advances in Neural Information Processing Systems*, 37:115523–115562, 2024.
- Yichi Zhang, Daniel W Apley, and Wei Chen. Bayesian optimization for materials design with mixed quantitative and qualitative variables. *Scientific Reports*, 2020.
- Lucas Zimmer, Marius Lindauer, and Frank Hutter. Auto-pytorch tabular: Multi-fidelity metalearning for efficient and robust autodl. *IEEE Transactions on Pattern Analysis and Machine Intelligence*, 43(9):3079 – 3090, 2021.

A LLM USAGE DISCLOSURE

We used large language models (LLMs) to assist with writing and editing this paper (e.g., improving clarity and readability of drafts). LLMs were also used to help polish proofs, to facilitate experiment scripting, and to generate plotting code. All technical content, research ideas, and final implementations were developed, verified, and approved by the authors.

B THEORETICAL ANALYSIS AND CALCULATIONS

In the following lemma, we prove a point-wise lower bound on the expected improvement before stopping for our recommended pairing of PBGI/LogEIPC stopping rule paired with either PBGI or LogEIPC acquisition function.⁴

Lemma 1. *Let X be compact, and let $f : X \rightarrow \mathbb{R}$ be a random function with constant mean μ . Consider a Bayesian optimization algorithm that begins at some initial point $x_1 \in X$ with cost $C = c(x_1)$, acquires additional points using either the PBGI or LogEIPC acquisition function, and uses the PBGI/LogEIPC stopping rule. Let $\tau = \min_{t \geq 1} \{\sup_{x \in X} \alpha_t^{\text{LogEIPC}}(x) < 0\}$ be the algorithm's stopping time, and denote the posterior expected improvement function by $\alpha_t^{\text{EI}}(x) = \text{EI}_{f|x_{1:t}, y_{1:t}}(x; y_{1:t}^*)$. Then, $\alpha_t^{\text{EI}}(x_{t+1}) \geq c(x_{t+1})$ for all $t < \tau$.*

Proof. While stopping has not occurred, meaning $t < \tau$, by the stopping criteria definition we have $\max_{x \in X} \alpha_t^{\text{EI}}(x)/c(x) \geq 1$. Hence, there exists at least one point with $\alpha_t^{\text{EI}}(x)/c(x) \geq 1$. We now argue for each algorithm.

PBGI. For each x we defined a threshold $\alpha_t^{\text{PBGI}}(x)$ by $\text{EI}_{f|x_{1:t}, y_{1:t}}(x; \alpha_t^{\text{PBGI}}(x)) = c(x)$. Since $\text{EI}_{f|x_{1:t}, y_{1:t}}$ is increasing in its second argument,

$$y_{1:t}^* \geq \alpha_t^{\text{PBGI}}(x) \iff \alpha_t^{\text{EI}}(x)/c(x) \geq 1. \quad (12)$$

The existence of a point with ratio at least 1 therefore implies that the set $\mathcal{S}_t = \{x : y_{1:t}^* \geq \alpha_t^{\text{PBGI}}(x)\}$ is non-empty. PBGI chooses x_{t+1} with the *smallest* threshold, and thus

$$\alpha_t^{\text{EI}}(x_{t+1}) = \text{EI}_{f|x_{1:t}, y_{1:t}}(x_{t+1}; y_{1:t}^*) \geq \text{EI}_{f|x_{1:t}, y_{1:t}}(x_{t+1}; \alpha_t^{\text{PBGI}}(x_{t+1})) = c(x_{t+1}). \quad (13)$$

(Log)EIPC. By definition x_{t+1} maximizes $\log(\alpha_t^{\text{EI}}(x)/c(x))$ and $\alpha_t^{\text{EI}}(x)/c(x)$, hence $\alpha_t^{\text{EI}}(x_{t+1}) \geq c(x_{t+1})$.

Thus for *both* algorithms, we have

$$\alpha_t^{\text{EI}}(x_{t+1}) \geq c(x_{t+1}), \quad \text{for all } t < \tau. \quad (14)$$

□

We can now use Lemma 1 to prove the following theorem, where we show that our PBGI/LogEIPC stopping rule (paired with the PBGI or LogEIPC acquisition function) also achieves cost-adjusted simple regret no worse than a naive baseline—stopping-immediately (*Immediate*). Notably, this guarantee may not hold for other acquisition-stopping rule pairings. Moreover, in the worst case, this is the best guarantee we can hope for—for instance, the evaluation costs can be uniformly high and no point is worth evaluating.

Theorem 2. *Consider the setting, acquisition function, and stopping rule specified in Lemma 1. Let $U = \mu - \mathbb{E}[\min_{x \in X} f(x)] < \infty$, then the algorithm's expected cost-adjusted simple regret is bounded by*

$$\mathbb{E} \left[y_{1:\tau}^* - \min_{x \in X} f(x) + \sum_{t=1}^{\tau} c(x_t) \right] \leq \mathbb{E} \left[\underbrace{y_1 - \min_{x \in X} f(x) + c(x_1)}_{\text{cost-adjusted regret of immediate stopping}} \right] = U + C. \quad (11)$$

⁴In fact, any acquisition function (e.g., expected improvement-cost (EIC) (Hu et al., 2025)) that ensures the one-step expected improvement is worth the evaluation cost before the stopping time τ can apply here.

Proof. We treat the two algorithms—meaning, the two acquisition function and stopping rule pairs—together and write $\mathcal{F}_t = \sigma(\{x_i, y_i\}_{i=1}^t)$ for the filtration generated by the observations. Since we are minimizing, the one-step improvement after iteration t is $y_{1:t-1}^* - y_{1:t}^*$, where recall that $y_{1:t}^* = \min_{1 \leq i \leq t} y_i$. By our assumption about the random function f , $\mathbb{E}[y_{1:1}^*] = \mu$ and the quantity $y_{1:1}^* - \min_{x \in X} f(x)$ has finite expectation $U < \infty$. Denote the posterior expected improvement function as $\alpha_t^{\text{EI}}(x) = \text{EI}_{f|x_{1:t}, y_{1:t}}(x; y_{1:t}^*)$.

By Lemma 1, $c(x_t) \leq \alpha_{t-1}^{\text{EI}}(x_t)$ for all $t \leq \tau$. Set $\Delta_t = y_{1:t-1}^* - y_{1:t}^* \geq 0$ for $2 \leq t \leq \tau$. Conditional on \mathcal{F}_{t-1} and the choice of x_t , we have

$$\mathbb{E}[\Delta_t | \mathcal{F}_{t-1}, x_t] = \alpha_{t-1}^{\text{EI}}(x_t). \quad (15)$$

Taking expectations and summing up from 2 to τ ,

$$\begin{aligned} \mathbb{E}\left[\sum_{t=2}^{\tau} \alpha_{t-1}^{\text{EI}}(x_t)\right] &= \mathbb{E}\left[\sum_{t=2}^{\infty} \mathbf{1}_{\{t \leq \tau\}} \alpha_{t-1}^{\text{EI}}(x_t)\right] \\ &= \mathbb{E}\left[\sum_{t=2}^{\infty} \mathbf{1}_{\{t \leq \tau\}} \mathbb{E}[\Delta_t | \mathcal{F}_{t-1}, x_t]\right] \\ &= \mathbb{E}\left[\sum_{t=2}^{\infty} \mathbf{1}_{\{t \leq \tau\}} \Delta_t\right] \quad (\text{tower property}) \\ &= \mathbb{E}\left[\sum_{t=2}^{\tau} \Delta_t\right] = \mathbb{E}[y_{1:1}^* - y_{1:\tau}^*]. \end{aligned} \quad (16)$$

Summing (14) over $t \leq \tau$, taking expectations, and applying (16), we have

$$\mathbb{E}\left[\sum_{t=2}^{\tau} c(x_t)\right] \leq \mathbb{E}\left[\sum_{t=2}^{\tau} \alpha_{t-1}^{\text{EI}}(x_t)\right] \leq \mathbb{E}[y_{1:1}^* - y_{1:\tau}^*]. \quad (17)$$

Adding the term $y_{1:\tau}^*$ on both sides of (17) gives

$$\mathbb{E}\left[y_{1:\tau}^* + \sum_{t=2}^{\tau} c(x_t)\right] \leq \mathbb{E}[y_{1:1}^*].$$

Finally, adding $c(x_1)$ to both sides and subtracting $\mathbb{E}[\min_{x \in X} f(x)]$ yields

$$\begin{aligned} \mathbb{E}\left[y_{1:\tau}^* - \min_{x \in X} f(x) + \sum_{t=1}^{\tau} c(x_t)\right] &\leq \mathbb{E}\left[y_{1:1}^* - \min_{x \in X} f(x) + c(x_1)\right] \\ &= \mathbb{E}\left[y_1 - \min_{x \in X} f(x) + c(x_1)\right] \\ &= \mu - \mathbb{E}\left[\min_{x \in X} f(x)\right] + \mathbb{E}[c(x_1)] \\ &= U + C, \end{aligned}$$

since $\mathbb{E}[y_1] = \mu$, $C = c(x_1)$, and $U = \mu - \mathbb{E}[\min_{x \in X} f(x)]$. This is exactly (11). \square

Corollary 3. Consider the setting, acquisition function, stopping rule, and notation specified in Lemma 1 and Theorem 2, but with costs rescaled by a factor $\lambda > 0$: both acquisition values and stopping conditions are computed using $\lambda c(\cdot)$. If the cost-scaling factor is set to $\lambda = \frac{U}{B-C}$, then the algorithm's expected cumulative unscaled cost satisfies $\mathbb{E}[\sum_{t=1}^{\tau} c(x_t)] \leq B$.

Proof. Since the Bayesian optimization algorithm considers the post-scaling cost, by Theorem 2 and the fact that $y_{1:\tau}^* - \min_{x \in X} f(x) > 0$ pointwise, we have

$$\mathbb{E}\left[\sum_{t=1}^{\tau} \lambda \cdot c(x_t)\right] \leq \mathbb{E}\left[y_{1:\tau}^* - \min_{x \in X} f(x) + \sum_{t=1}^{\tau} \lambda \cdot c(x_t)\right] \leq \mu - \mathbb{E}\left[\min_{x \in X} f(x)\right] + \lambda C = U + \lambda C. \quad (18)$$

Since $\lambda = U/(B - C)$, we have

$$\mathbb{E} \left[\sum_{t=1}^{\tau} c(x_t) \right] \leq \frac{U + \lambda C}{\lambda} = \frac{U}{\lambda} + C = B.$$

□

Note 4. In this paper, we focus on the setting where f is drawn from a Gaussian process, i.e., $f \sim \mathcal{GP}(\mu, K)$. In this case, the term $U = \mu - \mathbb{E}[\min_{x \in X} f(x)]$ can be further bounded above using classical results on the expected supremum/infimum of Gaussian processes; see, for example, Lifshits (2012, Theorem 10.1).

C EXPERIMENTAL SETUP

All experiments are implemented based on BoTorch (Balandat et al., 2020). Each Bayesian optimization procedure is initialized with $2(d + 1)$ random samples, where d is the dimension of the search domain. For Bayesian regret experiments, we follow the standard practice to generate the initial random samples using a quasirandom Sobol sequence. For empirical experiments, we randomly sample configuration IDs from a fixed pool of candidates—2,000 for LCBench and 32,768 for NATS-Bench. All computations are performed on CPU.

Each experiment is repeated with 50 random seeds, and we report the mean with error bars, given by two times the standard error, for each stopping rule. We also impose a cap on the number of iterations: 100 for 1D Bayesian regret, 500 for 8D Bayesian regret, and 200 for empirical experiments. If a stopping rule is not triggered before reaching this cap, we treat the stopping time as equal to the cap.

Gaussian process models. For all experiments, we follow the standard practice to apply Matérn kernels with smoothness $5/2$ and length scales learned from data via maximum marginal likelihood optimization, and standardize input variables to be in $[0, 1]^d$. For empirical experiments, we standardize output variables to be zero-mean and unit-variance, but not for Bayesian regret experiments. In this work, we consider the noiseless setting and set the fixed noise level to be 10^{-6} . In the unknown-cost experiments, we follow Astudillo et al. (2021) to model the objective and the logarithm of the cost function using independent Gaussian processes.

Acquisition function optimization. For the 1D Bayesian regret experiments, we optimize over 10,001 grid points. For the 8D Bayesian regret experiment, we use BoTorch’s ‘gen_candidates_torch’, a gradient-based optimizer for continuous acquisition function maximization, as it avoids reproducibility issues caused by internal randomness in the default scipy optimizer. For the empirical experiments, since LCBench and NATS-Bench provide only 2,000 and 32,768 configurations respectively, we optimize the acquisition function by simply applying an argmin/argmax over the acquisition values of the unevaluated configurations, without using any gradient-based methods.

Acquisition function and stopping rule parameters. For PBGI, we follow Xie et al. (2024) to compute the Gittins indices using 100 iterations of bisection search without any early stopping or other performance and reliability optimizations.

For UCB/LCB-based acquisition functions and stopping rules, we follow the original GP-UCB paper Srinivas et al. (2009) and the choice in UCB/LCB based stopping rules (Makarova et al., 2022; Ishibashi et al., 2023) to use the schedule $\beta_t = 2 \log(dt^2\pi^2/6\delta)$, where d is the dimension. We also adopt their choice of $\delta = 10^{-1}$ and a scale-down factor of 5.

For SRGap-med, which stops when the simple regret gap falls below χ times the median of its initial $T = 20$ values, we set $\chi = 0.1$ in the empirical experiments, instead of the default value $\chi = 0.01$ recommended in the literature. This adjustment was made because SRGap-med tends to stop too late on the LCBench datasets, likely due to the relatively small initial regret values and insignificant drop over time.

For PRB, we follow Wilson (2024) to use the schedule $N_t = \max(\lceil 64 * 1.5^{t-1} \rceil, 1000)$ for number of posterior samples, risk tolerance $\delta = 0.05$. The error bound ϵ is set to be 0.1 for Bayesian regret

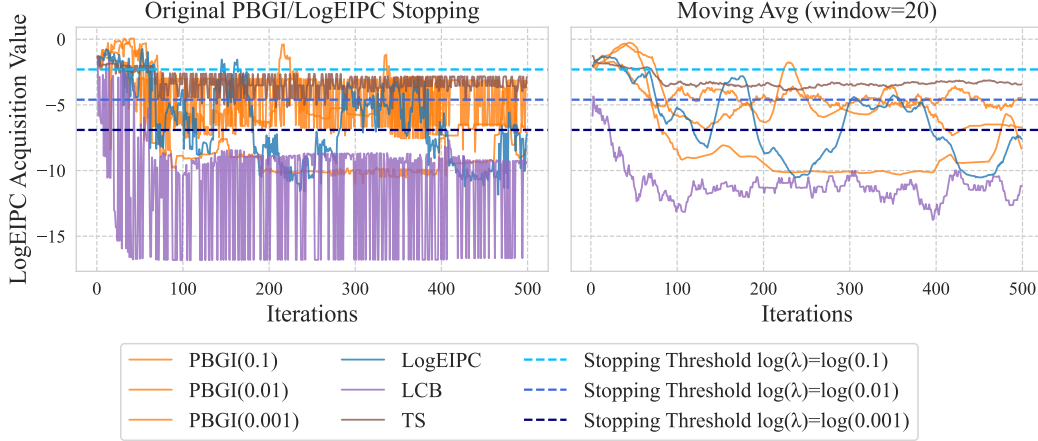


Figure 5: Comparison of the raw and moving-averaged PBGI/LogEIPC stopping rule statistics (i.e., the LogEIPC acquisition values) in Bayesian regret 8D experiments for multiple acquisition functions, with linear cost and stopping thresholds at $\log(0.1)$, $\log(0.01)$ and $\log(0.001)$. *Left:* The unaveraged statistic exhibits large, high-frequency fluctuations due to the difficulty of acquisition optimization in high dimensions. *Right:* Applying moving average (window=20) smooths these wiggles, yielding a more stable stopping signal.

experiments and 0.5% of the best test error (here, the misclassification rate) among all configurations for the empirical experiments.

For the 8D Bayesian regret experiments, we apply moving average over 20 iterations to mitigate oscillations in the optimizer. Figure 5 illustrates the challenges these oscillations pose when computing stopping rule statistics and shows the improvement with moving average. For consistency, we also apply 20-iteration averaging to the GSS and Convergence baselines.

Omitted baselines. We omit the KG acquisition function and stopping rule due to its high computational cost, as they are shown to be computationally intensive in the runtime experiments of Xie et al. (2024).

Objective functions: Bayesian regret. In all Bayesian regret experiments, each objective function f is sampled from a Gaussian process prior with a Matérn 5/2 kernel and a length scale of 0.1, using a different seed in each of the 50 trials.

Objective functions: empirical. In the empirical experiments, the validation error (scaled out of 100) is used as the objective function during the Bayesian optimization procedure, while the cost-adjusted simple regret is reported based on the corresponding test error.

Cost functions: Bayesian regret. In Bayesian regret experiments, we consider three types of evaluation costs: uniform, linear, and periodic. These costs are normalized such that $\mathbb{E}_{x \in [0,1]^d} [c(x)]$ is approximately 1 and their expressions (prior to cost scaling) are given below.

In the *uniform* cost setting, each evaluation incurs a constant cost of 1.

In the *linear* cost setting, the cost increases proportionally with the average coordinate value of the input:

$$\text{linear_cost}(x) = \frac{1 + 20 \cdot \left(\frac{1}{d} \sum_{i=1}^d x_i \right)}{11}.$$

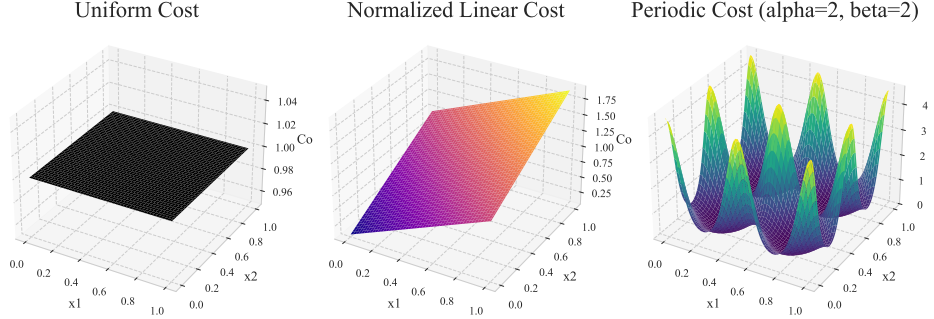


Figure 6: Surface plots of cost functions over $[0, 1]^2$: (Left) Uniform cost of 1 across domain. (Middle) Normalized linear cost increasing with the mean of x_1 and x_2 . (Right) Periodic cost with $\alpha = 2$, $\beta = 2$, normalized by Bessel-based factor.

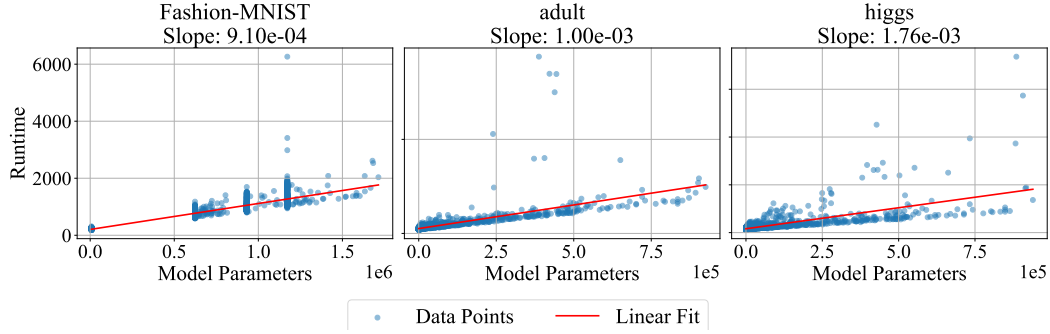


Figure 7: Empirical relationship between the number of model parameters and runtime for three LCBench datasets. Each subplot shows a scatter plot of actual runtime (y -axis) against number of model parameters (x -axis), along with a fitted linear regression line. The observed linear trend supports using 0.001 times the number of model parameters as a proxy for runtime. For *Fashion-MNIST* and *adult*, the fitted slopes are close to 0.001. The slope for *higgs* is slightly higher, possibly due to a few outliers.

In the *periodic* cost setting, the evaluation cost fluctuates across the domain. Following Astudillo et al. (2021), we define the periodic cost as

$$\text{periodic_cost}(x) = \frac{\exp\left(\frac{\alpha}{d} \sum_{i=1}^d \cos(2\pi\beta(x_i - x_i^*))\right)}{\left[I_0\left(\frac{\alpha}{d}\right)\right]^d},$$

where x_i^* denotes the coordinate of the global optimum of f , and I_0 is the modified Bessel function of the first kind, which acts as a normalization constant. We set $\alpha = 2$ and $\beta = 2$ to induce noticeable variation in cost across the domain, while ensuring that costly evaluations can still be worthwhile.

A visualization of the three cost functions is provided in Figure 6.

Cost functions: empirical. In the *unknown-cost* experiments, we treat runtime—meaning, the provided full model training time (200 epochs for LCBench and 90 epochs for NATS)—as evaluation costs (prior to cost scaling).

In the *known-cost* experiments, for LCBench, we use 0.001 times the number of model parameters as a proxy for runtime. This proxy is motivated by our observation of an approximately linear relationship between the number of model parameters and the actual runtime, with slope close to 0.001 (see Figure 7). Importantly, the number of model parameters can be computed in advance, before the Bayesian optimization procedure, based on the network structure and classification task, as we explain in detail below.

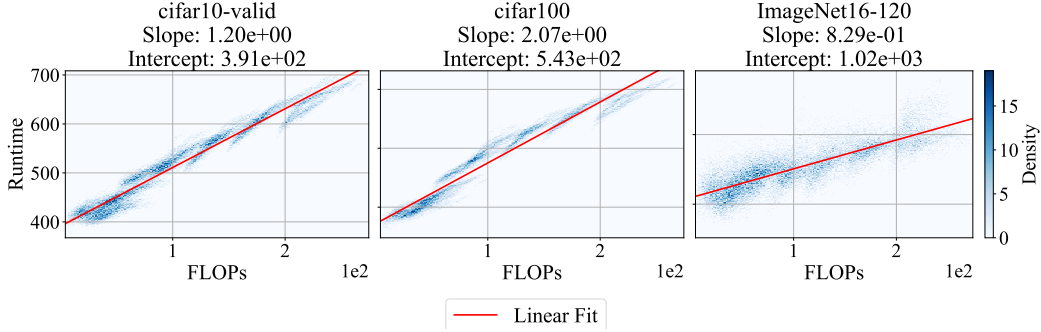


Figure 8: Empirical relationship between the number of FLOPs and runtime for the three NATS-Bench datasets. Each subplot shows a heatmap of actual runtime (y -axis) against number of FLOPs (x -axis), along with a fitted linear regression line. The observed linear trend supports using $\alpha \times \#FLOPs + \beta$ as a proxy for runtime.

In a feedforward neural network like shapedmlpnet with shape ‘funnel’, the model parameters are determined by input size (number of features), output size (e.g., number of classes), number of layers, size of each layer. The input size and output size are given by:

- Fashion-MNIST:
 - Input dimension: 784 (each image has 28×28 pixels, flattened into a vector of length 784)
 - Number of Output Features (output_feat): 10 (corresponding to 10 clothing categories)
- Adult:
 - Input Dimension: 14 (the dataset comprises 14 features, including both numerical and categorical attributes)
 - Number of Output Features: 1 (binary classification: income > 50K or $\leq 50K$)
- Higgs:
 - Input Dimension: 28 (each instance has 28 numerical features)
 - Number of Output Features: 1 (binary classification: signal or background process)

The number of layers (num_layers) and size of each layer (max_unit) can be obtained from the configuration. With these information, we can compute the total number of model parameters (weights and biases) based on the layer-wise structure as follows:

$$\text{layer_params}_{i \rightarrow i+1} = \text{layer}_i \cdot \text{layer}_{i+1} + \text{layer}_{i+1} \quad (\text{weights + biases}) \quad (19)$$

$$\text{model_params} = \sum_{i=0}^{L-1} \text{layer_params}_{i \rightarrow i+1} \quad (20)$$

$$\text{where } \text{layer}_0 = \text{input_dim}, \quad \text{layer}_L = \text{output_feat} \quad (21)$$

Similarly for NATS-Bench, we use $\alpha \times F + \beta$ as a proxy for runtime (see Figure 8 for a visualization of the linear relationship), where F is the number of floating point operations (FLOPs). Specifically, for *cifar10-valid*, we set $\alpha = 1, \beta = 400$; for *cifar100*, we set $\alpha = 2, \beta = 550$; and for *ImageNet16-120*, we set $\alpha = 1, \beta = 1000$.

FLOPs can also be computed in advance, as it is determined solely by the architecture’s structure and the fixed input shape. Specifically, they are precomputed and stored for each architecture. Since each architecture corresponds to a deterministic computational graph and all inputs (e.g., CIFAR-10 images) have a fixed shape, the FLOPs required for a forward pass can be calculated analytically—without executing the model on data.

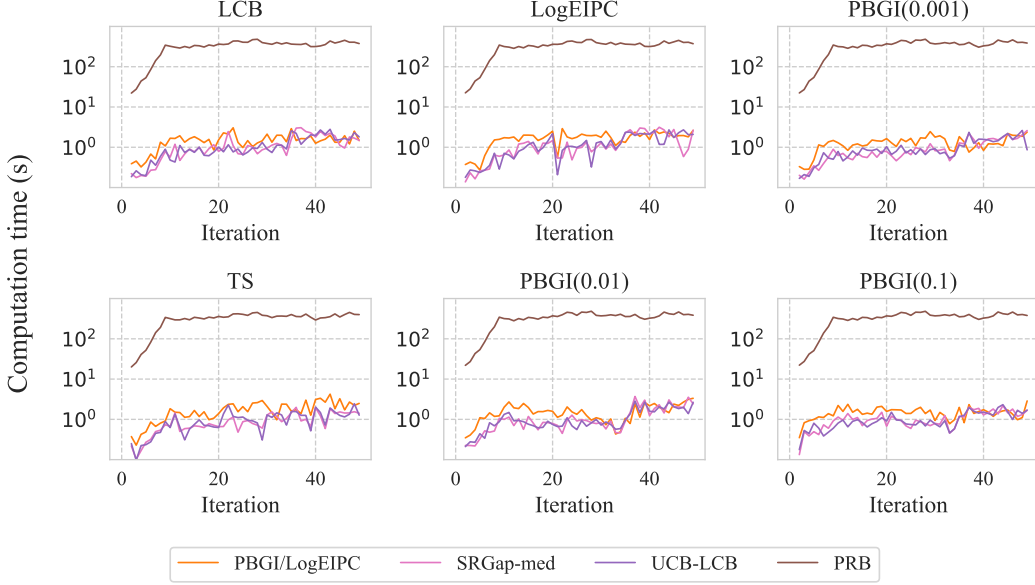


Figure 9: Evolution of per-iteration computation time (in log scale) for different stopping rules when paired with six acquisition policies on the 8-dimensional Bayesian regret benchmark. Each subplot shows the average runtime (in seconds) over 50 iterations under one acquisition function—LCB, Thompson Sampling, LogEIPC, PBGI($\lambda = 10^{-1}$), PBGI($\lambda = 10^{-2}$), and PBGI($\lambda = 10^{-3}$). Curves correspond to four stopping criteria: our PBGI/LogEIPC stopping rule, SRGap-med, UCB-LCB, and the probabilistic regret bound (PRB). Convergence and GSS can be applied using only the best observed value and thus require no additional computation time, thus they are omitted here. LogEIPC-med relies on the same underlying statistical computations as the LogEIPC rule, and therefore its runtime is not measured separately. The results show that PRB incurs significant computational overhead compared to other stopping rules.

D ADDITIONAL EXPERIMENT RESULTS

In this section, we present additional experimental results to further evaluate the performance of different acquisition-function-stopping-rule pairs across various settings. We also include alternative visualizations to aid interpretation of the results.

D.1 RUNTIME COMPARISON

First, we compare the runtime between our PBGI/LogEIPC stopping rule with several baselines. We measure the CPU time (in seconds) of the computation of the stopping rule, excluding the acquisition function computation and optimization.

From results in Figure 9 we can see that our PBGI/LogEIPC stopping rule is roughly as efficient as SRGap-med and UCB-LCB. In contrast, PRB is significantly more time-consuming, as it involves optimizing over up to 1000 samples.

D.2 ORDER OF STOPPING AND POSTERIOR UPDATES

Following the discussions in Section 3, we always compute our proposed stopping rule with respect to the optimal acquisition function value of the *next round*—namely, the one which is obtained after posterior updates have been performed. One could alternatively consider checking the stopping criteria *before* posterior updates, which is backward-looking rather than forward-looking. Figure 10 provides an empirical comparison between the two choices, showing that stopping *after* the posterior update leads to stronger empirical performance.

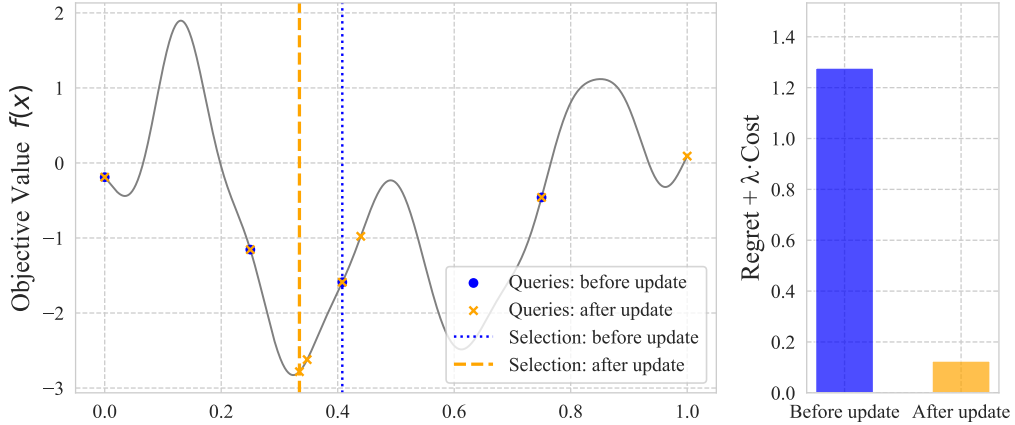


Figure 10: Illustration of a single draw from a Matérn-5/2 Gaussian process on $[0, 1]$ with lengthscale 0.1, optimized using PBGI acquisition function under uniform cost and cost-scaling factor $\lambda = 0.01$. We compare two variants of PBGI stopping rules: the *before-posterior-update* (this-round) stopping rule and the *after-posterior-update* (next-round) stopping rule. **Left:** The latent objective function (solid gray) and evaluation sequences for *before-posterior-update* stopping (blue circles) and *after-posterior-update* stopping (orange crosses). The dotted blue line and the dashed orange line mark the best observed value under each respective rule. **Right:** Cost-adjusted regret for each stopping rule. In this example, *after-posterior-update* stopping achieves strictly lower cost-adjusted regret despite performing more evaluations.

This suggests that the theoretical guarantee for the Gittins index policy in the correlated Pandora’s Box setting by Gergatsouli & Tzamos (2023), which is based on the *before-posterior-update* stopping, could potentially be improved by adopting the *after-posterior-update* stopping.

D.3 ADDITIONAL EXPERIMENT RESULTS: EMPIRICAL

This subsection presents additional experiment results on hyperparameter optimization over the three LCBench datasets and neural architecture size search over the three NATS datasets.

To isolate the effect of the acquisition function on cost-adjusted regret, we report the simple regret of several acquisition functions in the budgeted setting. We compare LogEIPC, PBGI, LCB, and TS, and additionally include PBGI-D with our recommended choice $\lambda_0 = U/(B - C)$ from Section 3.1.1, where $U = 50$ (reflecting the $[0, 100]$ range of classification accuracy) and $B - C = 10,000$ (corresponding to a budget after initial evaluation of 10,000 seconds, or roughly 3 hours). Cost-aware methods (LogEIPC and the PBGI variants) outperform cost-unaware ones (UCB and TS), with PBGI at smaller λ consistently better than LogEIPC. This mirrors the findings of Xie et al. (2024) and helps explain the strong performance of the matched PBGI combination in our main experiments.

Number of trials where stopping fails. We count the number of trials in which a stopping rule fails to trigger within our iteration cap of 200 and present the results in Table 1. From the table, we observe that on datasets from the NATS benchmark, regret-based and acquisition-based stopping rules—except for ours—often fail to stop early. On LCBench datasets, some regret-based stopping rules such as SRGap-med and UCB–LCB also frequently exceed the cap. In contrast, our stopping rule consistently stops early, which aligns with our theoretical result in Corollary 3.

Alternative visualization: cost-adjusted regret vs iteration. We provide an alternative visualization of cost-adjusted simple regret by plotting its mean and error bars at fixed iterations, along with the mean and error bars of the stopping iterations for each rule. This allows us to compare the performance of adaptive stopping rules not only against the hindsight-optimal adaptive stopping but also against the hindsight-optimal fixed-iteration stopping.

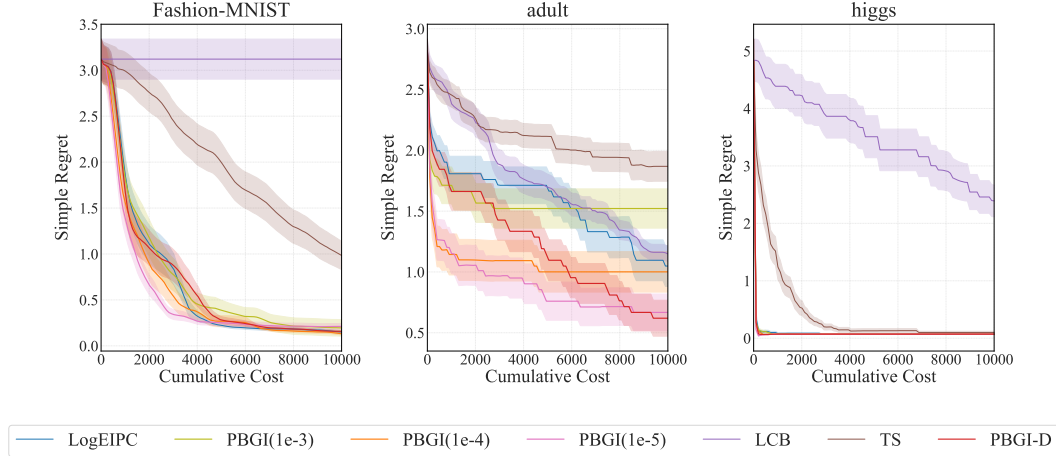


Table 1: Number of trials (out of 50) where each stopping rule failed to trigger within 200 iterations, for each dataset in the LC-Bench (first three) and NATS (last three) benchmarks and each acquisition function. Results are identical across acquisition functions.

| Dataset | PBGI | LogEIPC-med | SRGap-med | UCB-LCB | GSS | Convergence | PRB |
|---------------|------|-------------|-----------|---------|-----|-------------|-----|
| Fashion-MNIST | 0 | 0 | 0 | 50 | 0 | 0 | 0 |
| adult | 5 | 0 | 7 | 38 | 0 | 0 | 6 |
| higgs | 0 | 0 | 31 | 50 | 0 | 0 | 0 |
| Cifar10 | 0 | 32 | 50 | 50 | 0 | 0 | 26 |
| Cifar100 | 3 | 17 | 50 | 50 | 0 | 0 | 2 |
| ImageNet | 0 | 23 | 50 | 50 | 0 | 0 | 0 |

As shown in the empirical setting in Figures 12 to 17, cost-adjusted regret generally decreases in the early iterations and then increases. The turning point is exactly the hindsight-optimal fixed-iteration stopping point, and our PBGI/LogEIPC stopping rule consistently performs close to this optimum, particularly when paired with the PBGI acquisition function.

Cost model mismatch: proxy runtime vs actual runtime. In the known-cost setting of hyper-parameter tuning, a practical approach is to use a proxy for runtime as the evaluation cost during the Bayesian optimization procedure. In our case, we use the number of model parameters scaled by a constant factor, which can be known in advance and has been shown to correlate well with the actual runtime. However, for reporting performance, one may prefer to use the actual runtime to better reflect real-world cost. To assess the impact of this cost model mismatch, we compare the cost-adjusted simple regret obtained when evaluation costs are computed using either the proxy runtime or the actual runtime. As shown in Figure 18, our PBGI/LogEIPC stopping rule remains close to the hindsight optimal even when there is a mismatch, although its ranking may shift slightly (e.g., from best to second-best on the *higgs* dataset).

Unknown-cost. Astudillo et al. (2021, Proposition 2) proposed modeling unknown cost $c(x)$ via

$$\mathbb{E}[1/c(x)]^{-1} = \exp(\mu_{\ln c}(x) - (\sigma_{\ln c}(x))^2/2). \quad (22)$$

An alternative is

$$\mathbb{E}[c(x)] = \exp(\mu_{\ln c}(x) + (\sigma_{\ln c}(x))^2/2). \quad (23)$$

The difference in sign before the variance term reflects how each formulation handles predictive uncertainty: (22) encourages more exploration than (23). For PBGI under the unknown-cost setting,

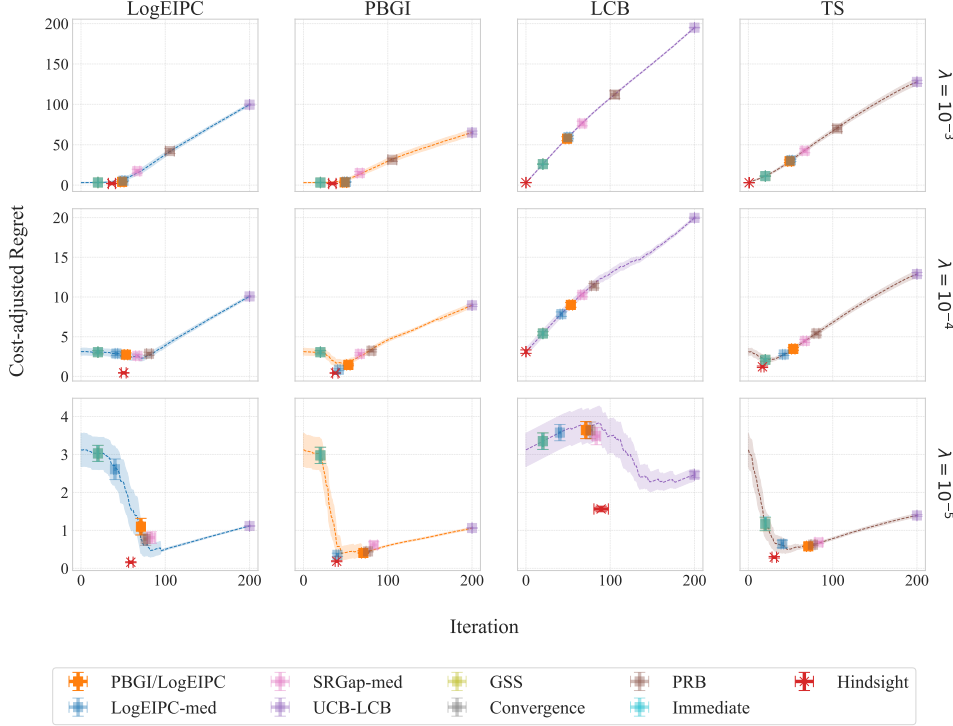


Figure 12: Comparison of cost-adjusted simple regret across acquisition function and stopping rule pairs on the *Fashion-MNIST* dataset. The objective function is the validation error, and the evaluation cost is the proxy runtime, scaled by three different cost-scaling factors $\lambda = 10^{-3}, 10^{-4}, 10^{-5}$. We can see that the PBGI/LogEIPC stopping rule consistently achieves cost-adjusted regret close to the hindsight optimal adaptive stopping as well as the hindsight optimal fixed-iteration stopping when paired with the PBGI acquisition function, though not always the best.

it is more natural to replace $c(x)$ in (5) with $\mathbb{E}[c(x)]$ using (23), as this aligns with how costs enter the root-finding problem. For LogEIPC, both variants are possible—we refer to the (22) version as *LogEIPC-inv* and the (23) version as *LogEIPC-exp*. However, equivalence between PBGI and LogEIPC stopping rules and our theoretical guarantees hold only with (23) but not with (22). Accordingly, we use (23) for both methods in our experiments to maintain consistency and preserve this equivalence. Figure 19 shows performance of acquisition function and stopping rule pairs under the unknown-cost setting, which are qualitatively similar to the known-cost setting.

D.4 ADDITIONAL EXPERIMENT RESULTS: BAYESIAN REGRET

In this section, we present the complete Bayesian regret results. Figures 20 to 22 show the 1D experiments, and Figures 23 to 25 show the 8D experiments. Each figure corresponds to one cost setting (uniform, linear or periodic) and three values of the cost-scaling factor, $\lambda = 10^{-1}, 10^{-2}, 10^{-3}$. In all of the experimental results, we observe that PBGI/LogEIPC acquisition function + PBGI/LogEIPC stopping achieves cost-adjusted regret that is not only competitive with the baselines, but is also competitive regarding the *best in hindsight* fixed iteration stopping and often competitive even comparing to *hindsight optimal* stopping. These results indicate that our automatic stopping rule can replace manual selection of stopping times without loss in performance. Figures 20 to 25 also show that our PBGI/LogEIPC stopping rule outperforms other baselines when the cost-scaling factor λ is large, indicating that it's an especially suitable stopping criteria when evaluation is expensive.

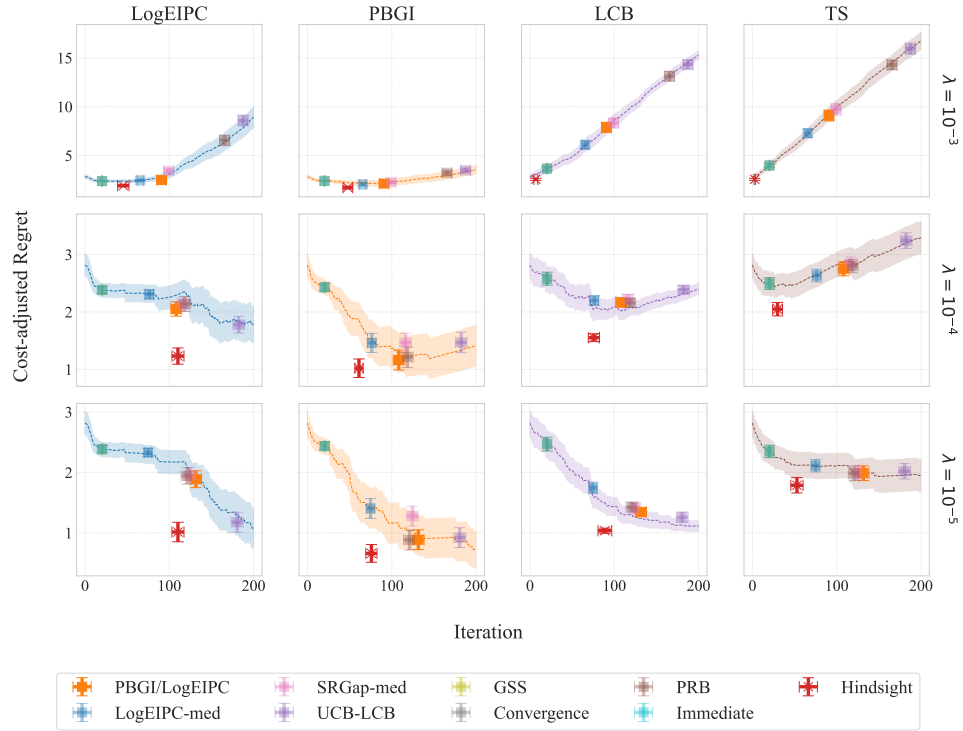


Figure 13: Comparison of cost-adjusted simple regret across acquisition function and stopping rule pairs on the *adult* dataset. The objective function is the validation error, and the evaluation cost is the proxy runtime, scaled by three different cost-scaling factors $\lambda = 10^{-3}, 10^{-4}, 10^{-5}$. We can see that the PBGI/LogEIPC stopping rule consistently achieves the cost-adjusted regret close to hindsight optimal adaptive stopping and hindsight optimal fixed-iteration stopping when paired with the PBGI or TS acquisition function, particularly with PBGI.

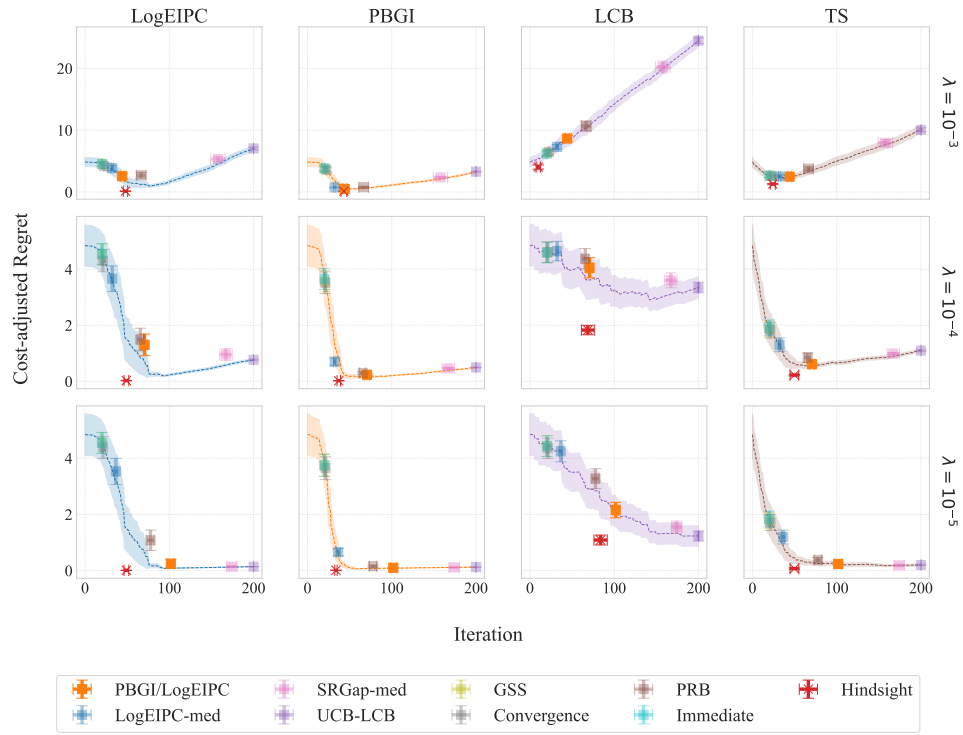


Figure 14: Comparison of cost-adjusted simple regret across acquisition function and stopping rule pairs on the *higgs* dataset. The objective function is the validation error, and the evaluation cost is the proxy runtime, scaled by three different cost-scaling factors $\lambda = 10^{-3}, 10^{-4}, 10^{-5}$. We can see that the PBGI/LogEIPC stopping rule consistently achieves the best cost-adjusted regret when paired with the LogEIPC, PBGI, or TS acquisition function, particularly with PBGI. These pairs not only approach the hindsight optimal adaptive stopping but also perform comparably to the hindsight optimal fixed-iteration stopping.

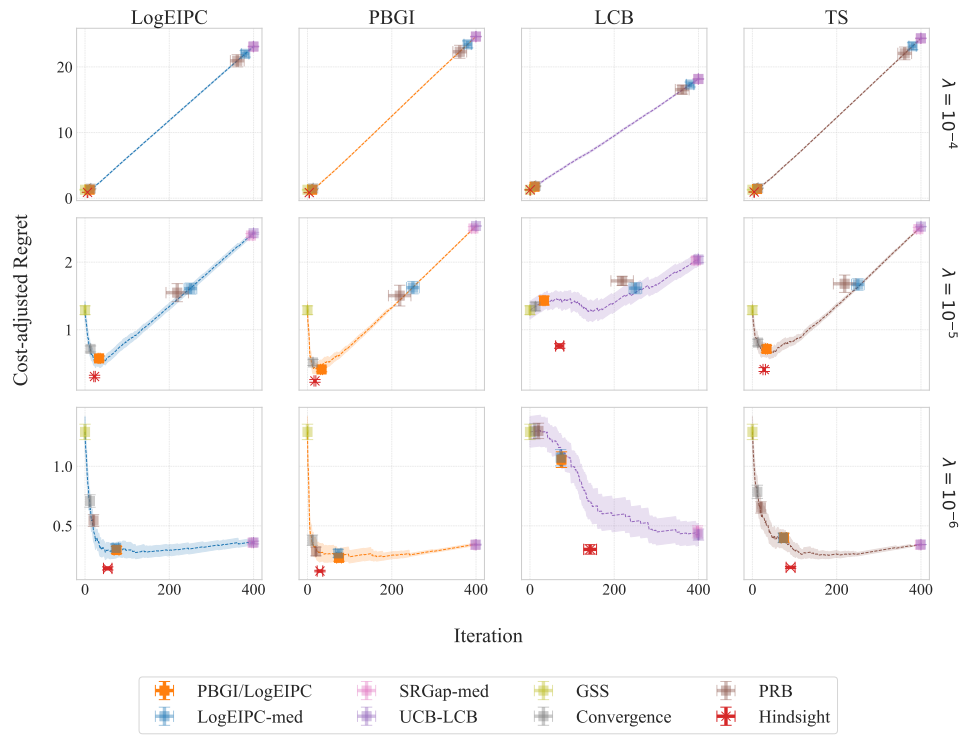


Figure 15: Comparison of cost-adjusted simple regret across acquisition function and stopping rule pairs on the *cifar10-valid* dataset. The objective function is the validation error, and the evaluation cost is the proxy runtime, scaled by three different cost-scaling factors $\lambda = 10^{-4}, 10^{-5}, 10^{-6}$. We can see that the PBGI/LogEIPC stopping rule consistently achieves the best cost-adjusted regret when paired with the LogEIPC, PBGI, or TS acquisition function, particularly with PBGI. These pairs not only approach the hindsight optimal adaptive stopping but also perform comparably to the hindsight optimal fixed-iteration stopping.

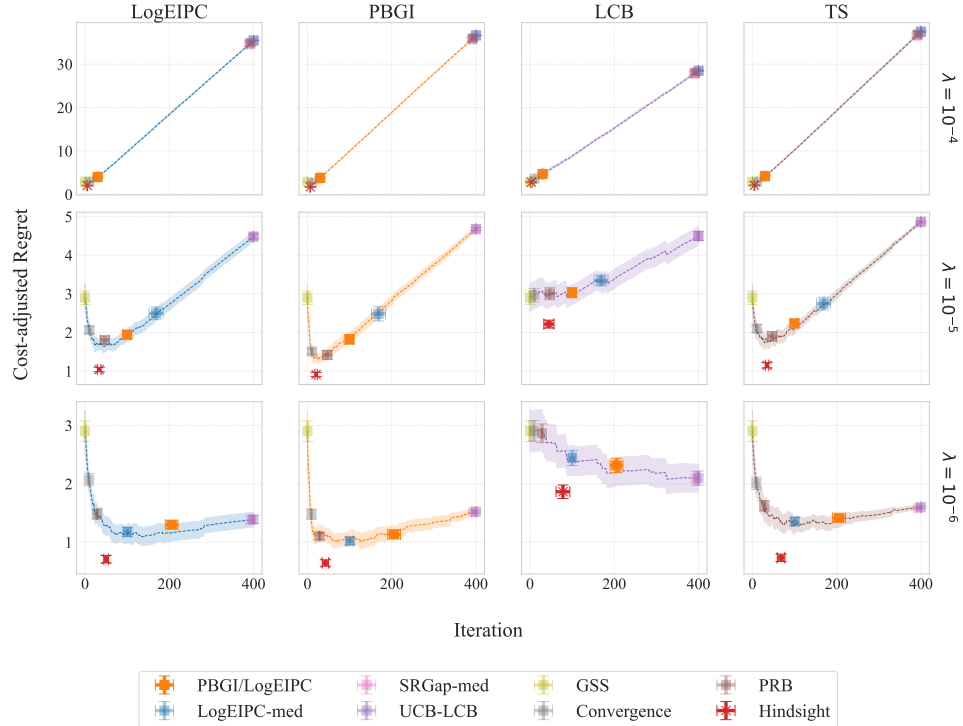


Figure 16: Comparison of cost-adjusted simple regret across acquisition function and stopping rule pairs on the *cifar100* dataset. The objective function is the validation error, and the evaluation cost is the proxy runtime, scaled by three different cost-scaling factors $\lambda = 10^{-4}, 10^{-5}, 10^{-6}$. The PBGI/LogEIPC stopping rule remains competitive at $\lambda = 10^{-4}$ and 10^{-6} , though not always the best. At $\lambda = 10^{-5}$, unlike in most experiments, it stops noticeably late (though still outperforming several other rules), even when paired with its matching acquisition function. By Lemma 1, under model match, the PBGI/LogEIPC rule with the corresponding acquisition function should never incur negative expected cost-adjusted regret before stopping. The suboptimal behavior observed here points to significant model mismatch on the *cifar100* dataset.

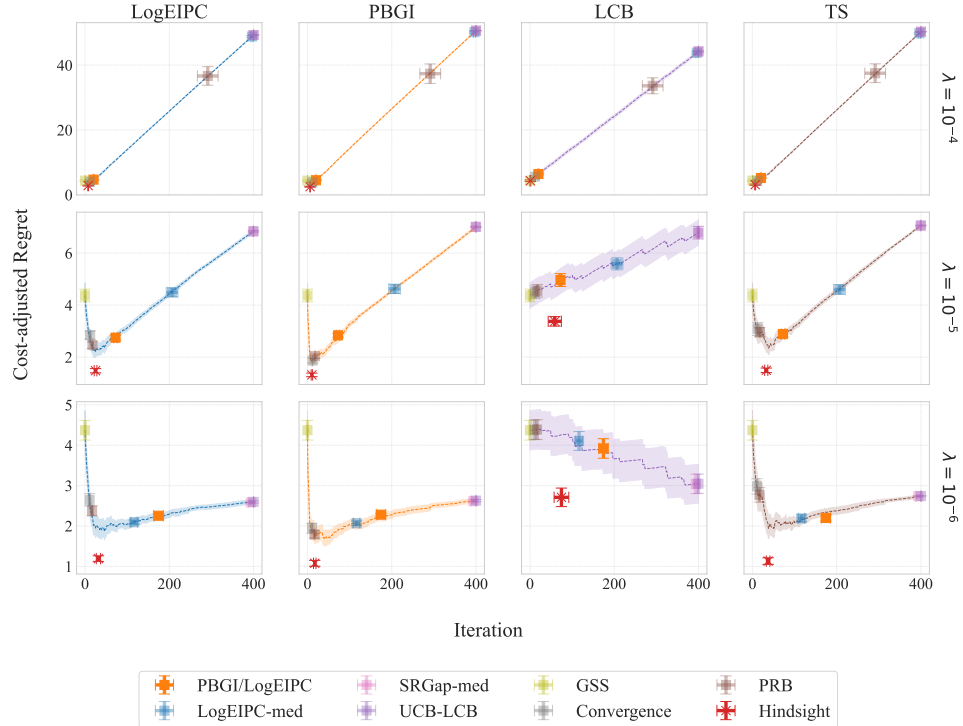


Figure 17: Comparison of cost-adjusted simple regret across acquisition function and stopping rule pairs on the *ImageNet16-120* dataset. The objective function is the validation error, and the evaluation cost is the proxy runtime, scaled by three different cost-scaling factors $\lambda = 10^{-4}, 10^{-5}, 10^{-6}$. The PBGI/LogEIPC stopping rule remains competitive at $\lambda = 10^{-4}$ and 10^{-6} , though not always the best. At $\lambda = 10^{-5}$, unlike in most experiments, it stops noticeably late (though still outperforming several other rules), even when paired with its matching acquisition function. By Lemma 1, under model match, the PBGI/LogEIPC rule with the corresponding acquisition function should never incur negative expected cost-adjusted regret before stopping. The suboptimal behavior observed here points to significant model mismatch on the *ImageNet16-120* dataset.

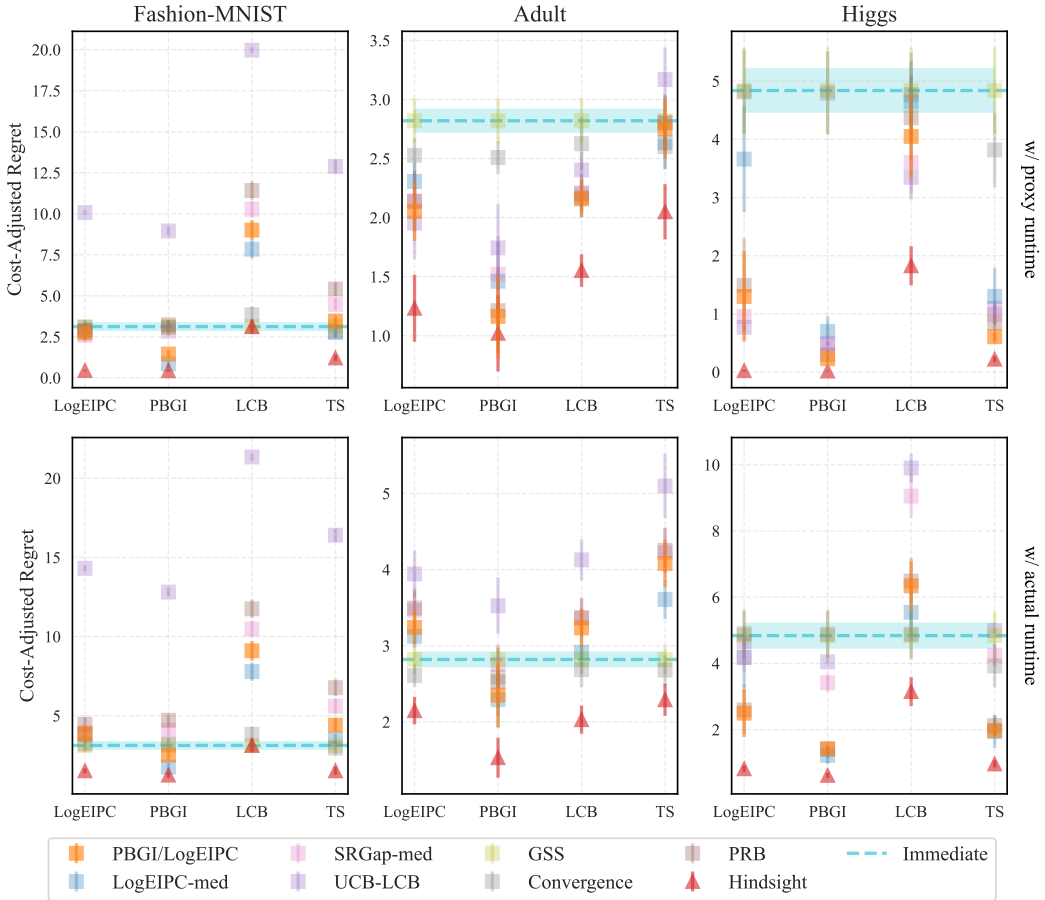


Figure 18: Comparison of cost-adjusted simple regret on LC-Bench with $\lambda = 10^{-4}$, using scaled proxy runtime vs. scaled actual runtime as evaluation cost. While our PBGI/LogEIPC stopping rule performs slightly worse under actual runtime (e.g., dropping from best to second-best on the *higgs* dataset), likely due to cost model mismatch, it remains close to the hindsight optimal in all cases.

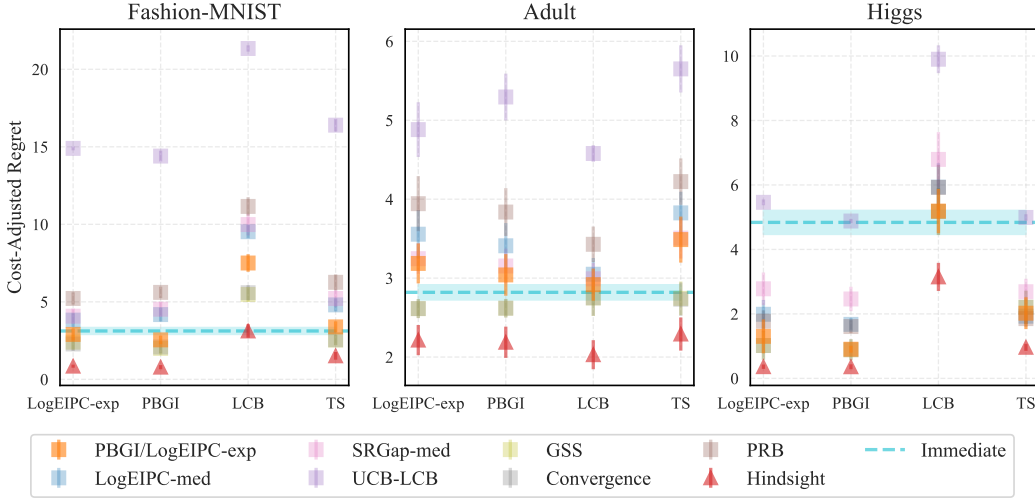


Figure 19: Comparison of cost-adjusted simple regret across acquisition function and stopping rule pairs under the unknown-cost setting on LCBench with $\lambda = 10^{-4}$. Our PBGI/LogEIPC stopping rule remains close to the hindsight optimal when paired with the LogEIPC-exp or PBGI acquisition function, sometime slightly worse then heuristics such as GSS and Convergence. It is also slightly worse than Immediate on *Adult*, probably due to a cost-model mismatch under the unknown-cost setting.

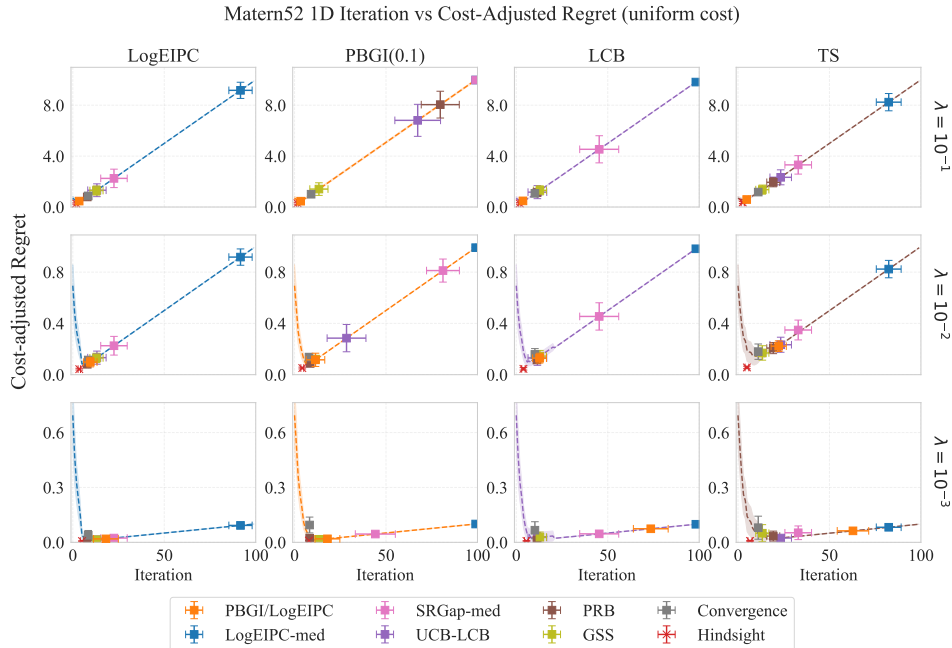


Figure 20: Comparison of cost-adjusted simple regret across acquisition function and stopping rule pairs in the 1D Bayesian regret experiments, with cost-scaling factor $\lambda = 10^{-1}, 10^{-2}, 10^{-3}$ and under uniform cost. The dashed line in each subplot represent fixed iteration stopping (e.g., the y-axis value of the line at iteration 50 represent the cost-adjusted regret when always stopping at iteration 50).

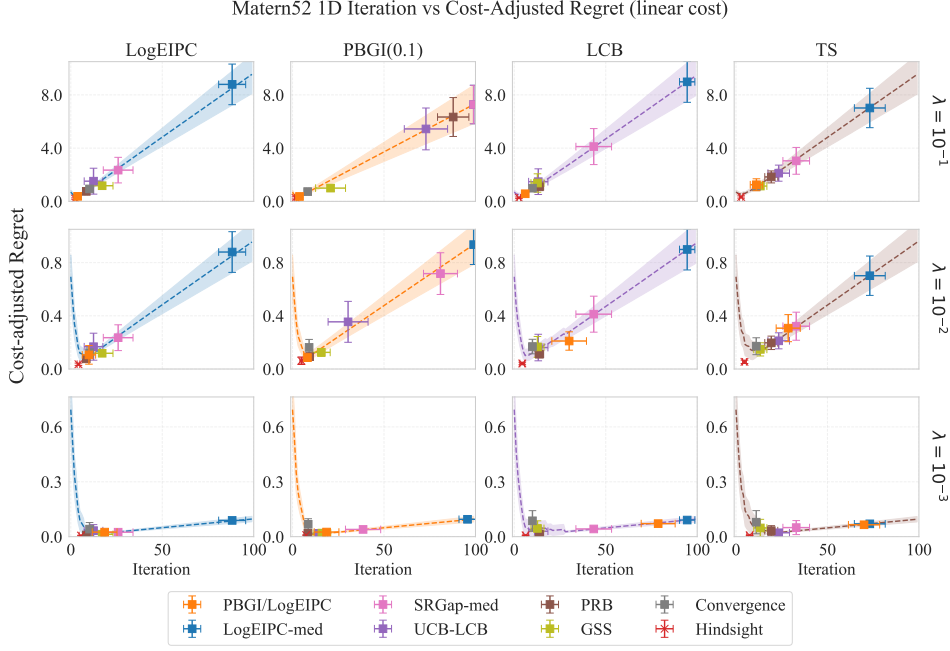


Figure 21: Comparison of cost-adjusted simple regret across acquisition function and stopping rule pairs in the 1D Bayesian regret experiments, with cost-scaling factor $\lambda = 10^{-1}, 10^{-2}, 10^{-3}$ and under linear cost. The dashed line in each subplot represent fixed iteration stopping (e.g., the y-axis value of the line at iteration 50 represent the cost-adjusted regret when always stopping at iteration 50).

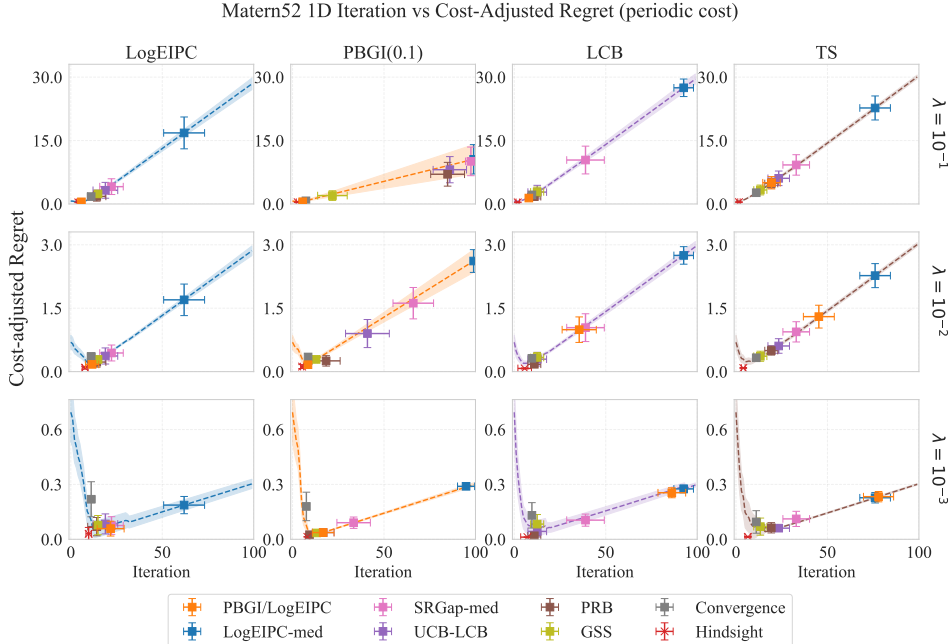


Figure 22: Comparison of cost-adjusted simple regret across acquisition function and stopping rule pairs in the 1D Bayesian regret experiments, with cost-scaling factor $\lambda = 10^{-1}, 10^{-2}, 10^{-3}$ and under periodic cost. The dashed line in each subplot represent fixed iteration stopping (e.g., the y-axis value of the line at iteration 50 represent the cost-adjusted regret when always stopping at iteration 50).

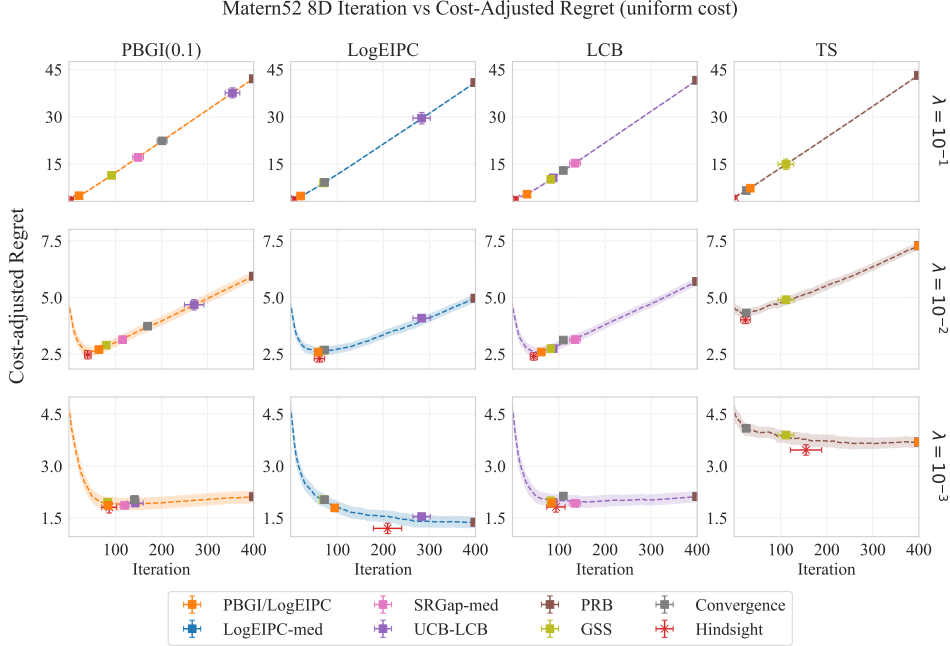


Figure 23: Comparison of cost-adjusted simple regret across acquisition function and stopping rule pairs in the 8D Bayesian regret experiments, with cost-scaling factor $\lambda = 10^{-1}, 10^{-2}, 10^{-3}$ and under uniform cost. The dashed line in each subplot represent fixed iteration stopping (e.g., the y-axis value of the line at iteration 50 represent the cost-adjusted regret when always stopping at iteration 50).

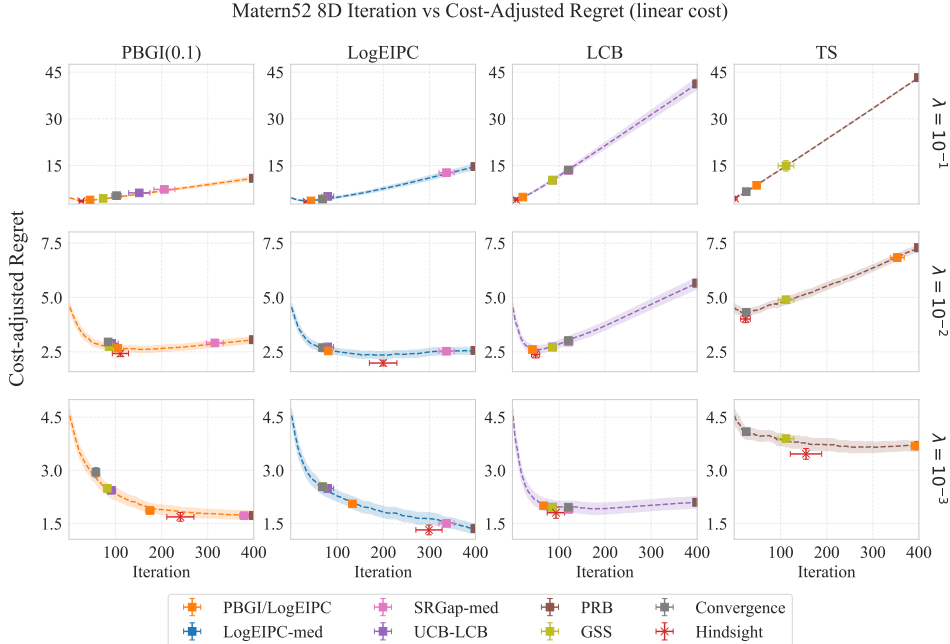


Figure 24: Comparison of cost-adjusted simple regret across acquisition function and stopping rule pairs in the 8D Bayesian regret experiments, with cost-scaling factor $\lambda = 10^{-1}, 10^{-2}, 10^{-3}$ and under linear cost. The dashed line in each subplot represent fixed iteration stopping (e.g., the y-axis value of the line at iteration 50 represent the cost-adjusted regret when always stopping at iteration 50).

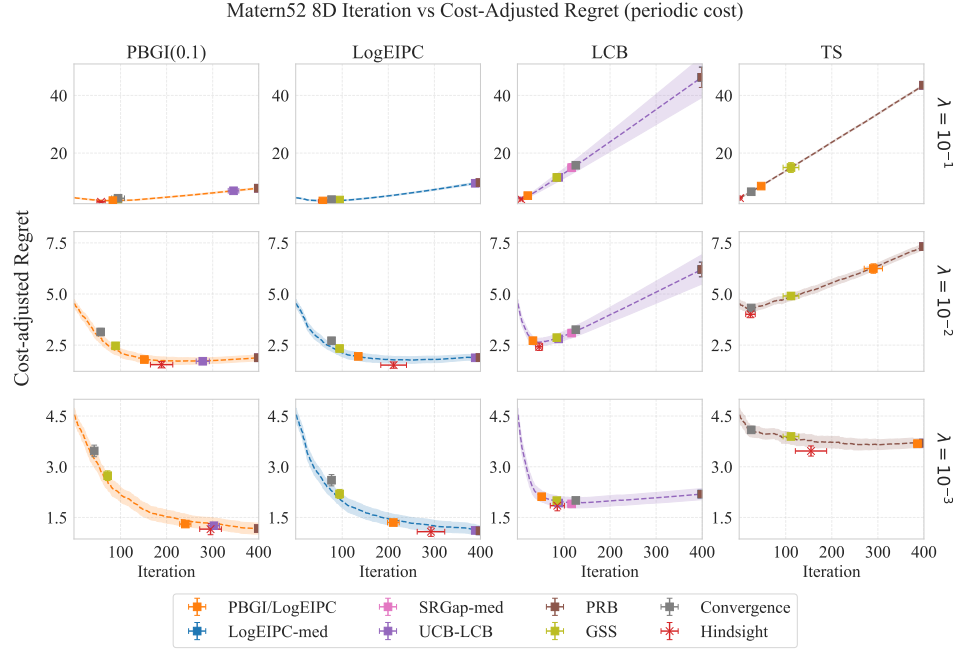


Figure 25: Comparison of cost-adjusted simple regret across acquisition function and stopping rule pairs in the 8D Bayesian regret experiments, with cost-scaling factor $\lambda = 10^{-1}, 10^{-2}, 10^{-3}$ and under periodic cost. The dashed line in each subplot represent fixed iteration stopping (e.g., the y-axis value of the line at iteration 50 represent the cost-adjusted regret when always stopping at iteration 50).